

Large Water Plume Deposits on Europa are Short Lived

Marina Casado Anarte¹, Hans Huybrighs², Sebastian Cervantes³, Christina Plainaki⁴, Lynnae C. Quick⁵, Stephenie Brophy Lee⁶, Isabelle Ledwidge⁷, and Noa Vigouroux⁸

¹Dublin Institute for Advanced Studies Dunsink Observatory

²Dublin Institute For Advanced Studies

³Dublin Institute for Advanced Studies, DIAS Dunsink Observatory

⁴Max Planck Institute for Solar System Research

⁵NASA Goddard Space Flight Center

⁶Dublin Institute for Advance Studies

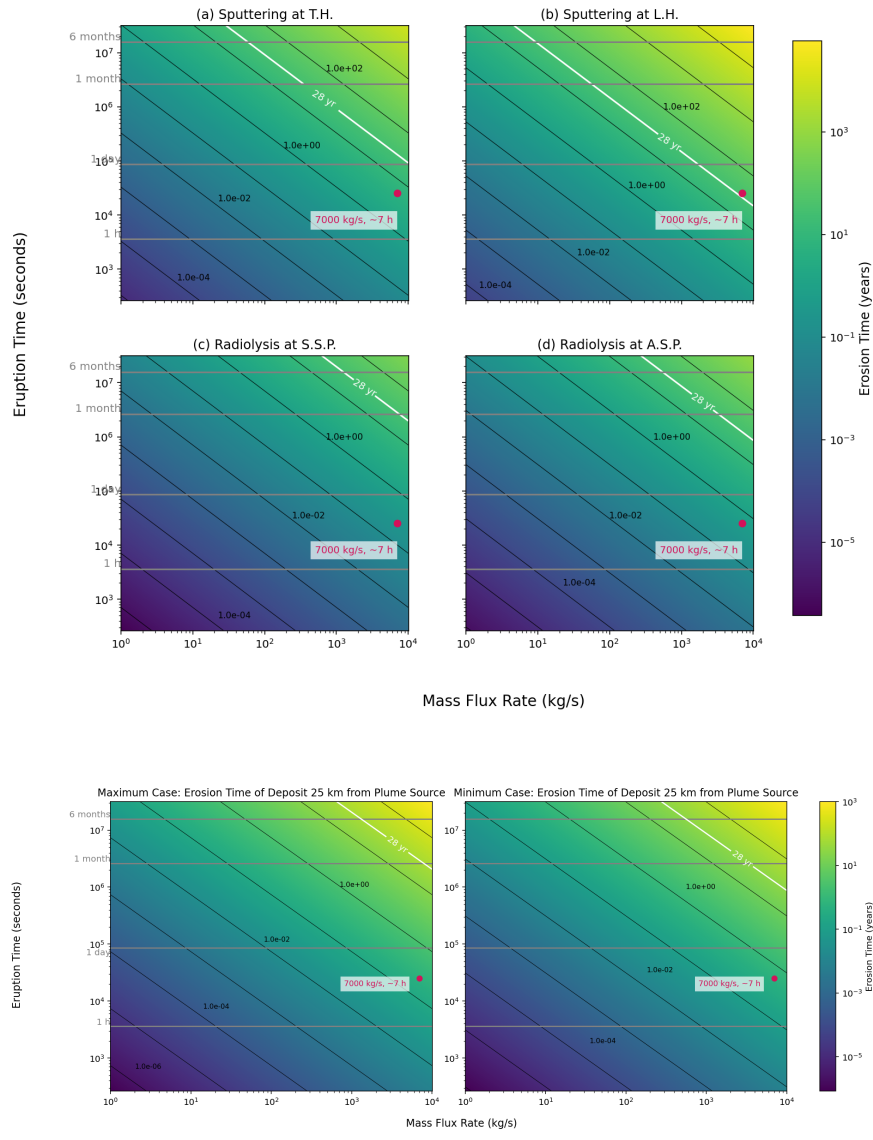
⁷Trinity College Dublin

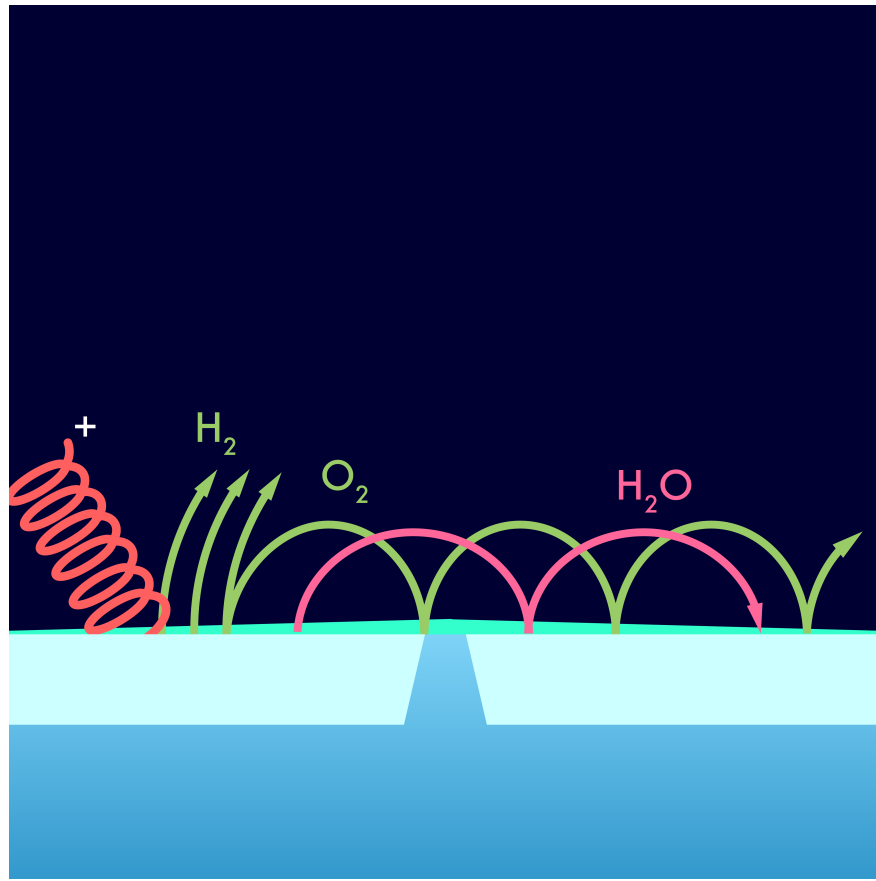
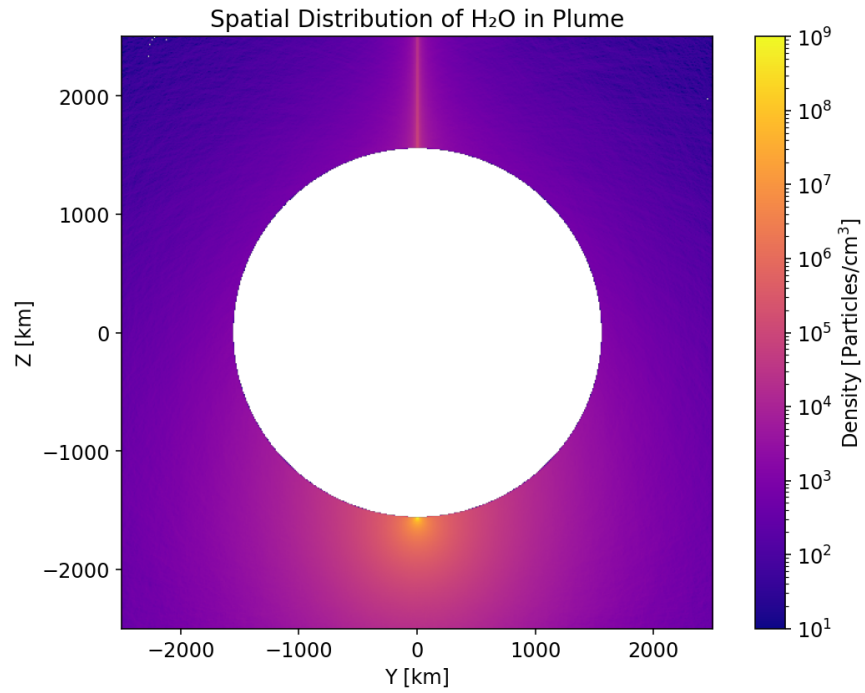
⁸University College Dublin

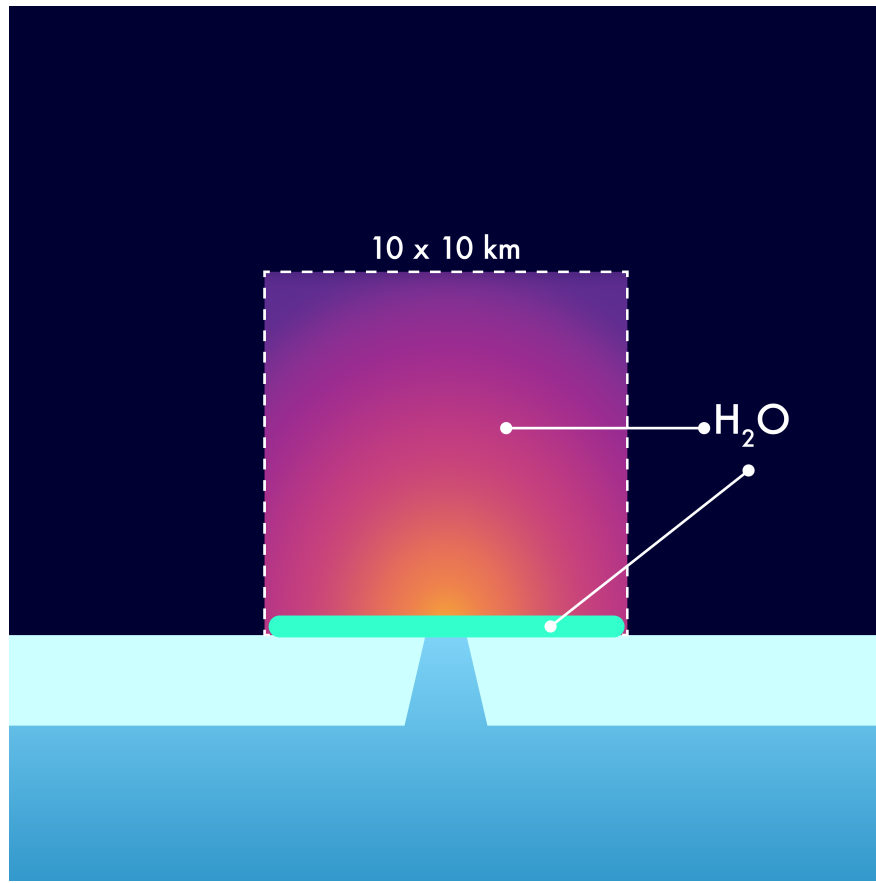
September 02, 2025

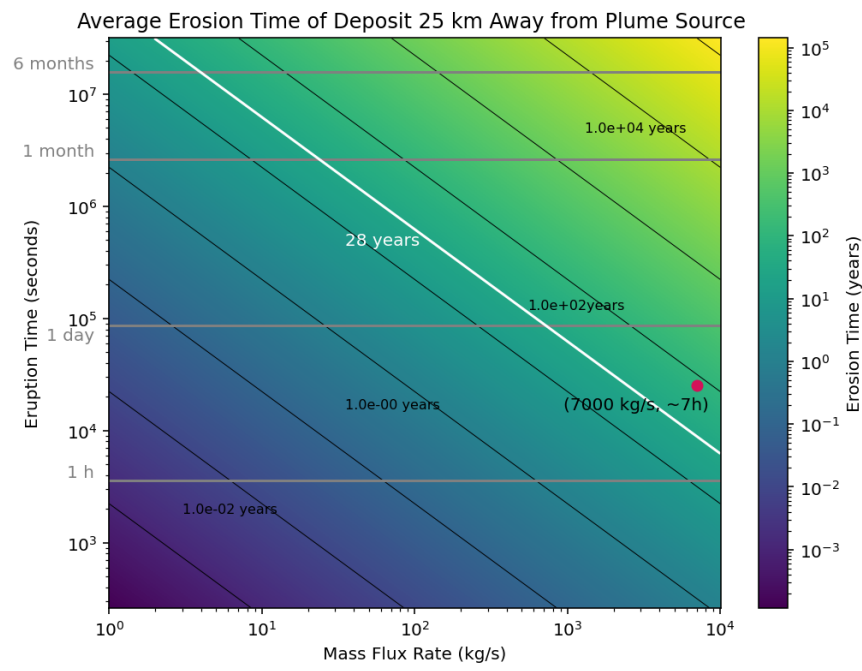
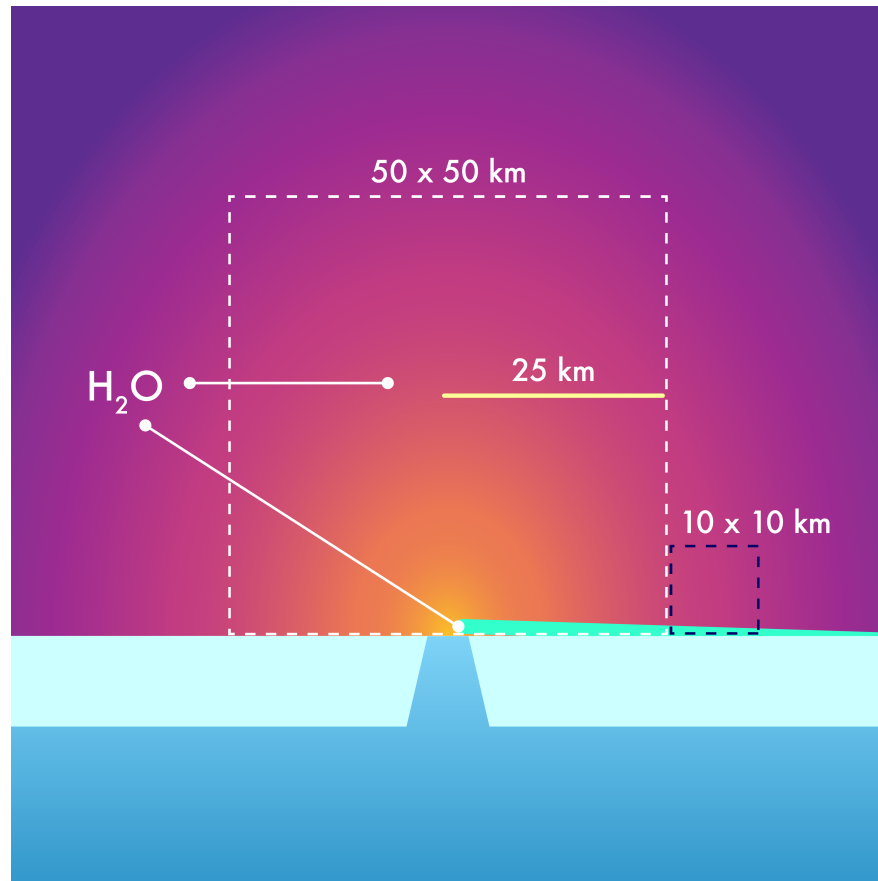
Abstract

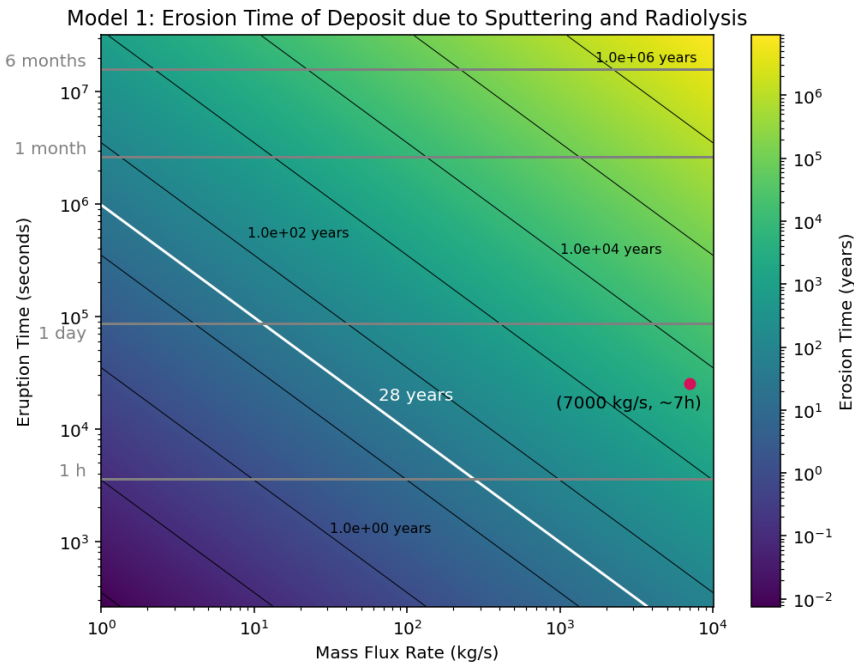
We investigate the transient nature of water plume deposits on Europa's surface, focusing on how radiolysis and ion sputtering (Europa's two most effective erosion processes) affect their lifetime. Our study is motivated by the lack of observed surface changes in imaging data, despite tentative plume detections, and aims to inform future missions, such as JUICE and Europa Clipper, about expected timescales of deposit survival to optimise their observational strategies. We present two models that simulate a first order estimate of the erosion time of deposits formed by water plumes considering a wide range of mass flux and eruption duration. Model 1 considers a confined (10 km) deposit near the source, while Model 2 evaluates the erosion material deposited 25 km from the plume source to match observation limitations in other studies. Our results show that plume deposits are short lived relative to Europa's average surface age for a wide range of mass fluxes and eruption times. Even intense plumes with $\$10\{,}000\$^{\sim}$ kg/s mass fluxes produce deposits that erode within $\sim 10\$^{\sim}$ Ma. For plumes such as the one observed by HST in 2012, deposits may be removed within years to decades. Erosion rates vary significantly with location, with polar regions offering the best conditions for long-term preservation. These findings support the hypothesis that the absence of visible deposits in current data may be due to rapid erosion rather than a lack of activity. They highlight the importance of time sensitive and geographically targeted observations for maximising the scientific output of upcoming missions.











Large Water Plume Deposits on Europa are Short Lived

M. Casado-Anarte^{1,2}, H. L. F. Huybrighs¹, S. Cervantes¹, C. Plainaki^{3,4}, L. C. Quick⁵, S. Brophy Lee¹, I. Ledwidge^{1,6}, N. Vigouroux^{1,7}

¹ Astronomy & Astrophysics Section, School of Cosmic Physics, Dublin Institute for Advanced Studies, DIAS Dunsink Observatory, Dublin D15 XR2R, Ireland

²Maynooth University, National University of Ireland Maynooth, Maynooth, Co.Kildare, Ireland

³Max Planck Institute for Solar System Research(MPS),Justus-von-Liebig-Weg 3, 37077 Göttingen, Germany.

⁴Italian Space Agency (ASI), Via del Politecnico snc, 00133 Rome, Italy

⁵NASA Goddard Space Flight Center, Greenbelt, MD, USA

⁶Trinity College Dublin, the University of Dublin, College Green, Dublin 2, D02 PN40, Ireland

⁷University College Dublin, Belfield, Dublin 4, Ireland

Key Points:

- Plume deposits ($\gtrsim 10$ km) on Europa are short-lived compared to its average surface age, making their detection difficult.
- Erosion rates are not uniform; local energetic ion environments significantly influence plume deposit survivability.
- To detect HST-type plume deposits before erosion, missions need camera resolution < 50 km and observations within months of deposition.

21 **Abstract**

22 We investigate the transient nature of water plume deposits on Europa's surface,
 23 focusing on how radiolysis and ion sputtering (Europa's two most effective erosion pro-
 24 cesses) affect their lifetime. Our study is motivated by the lack of observed surface changes
 25 in imaging data, despite tentative plume detections, and aims to inform future missions,
 26 such as JUICE and Europa Clipper, about expected timescales of deposit survival to op-
 27 timise their observational strategies.

28 We present two models that simulate a first order estimate of the erosion time of
 29 deposits formed by water plumes considering a wide range of mass flux and eruption du-
 30 ration. Model 1 considers a confined (10 km) deposit near the source, while Model 2 eval-
 31 uates the erosion material deposited 25 km from the plume source to match observation
 32 limitations in other studies.

33 Our results show that plume deposits are short lived relative to Europa's average
 34 surface age for a wide range of mass fluxes and eruption times. Even intense plumes with
 35 10,000 kg/s mass fluxes produce deposits that erode within ~ 10 Ma. For plumes such
 36 as the one observed by HST in 2012, deposits may be removed within years to decades.
 37 Erosion rates vary significantly with location, with polar regions offering the best con-
 38 ditions for long-term preservation.

39 These findings support the hypothesis that the absence of visible deposits in cur-
 40 rent data may be due to rapid erosion rather than a lack of activity. They highlight the
 41 importance of time sensitive and geographically targeted observations for maximising
 42 the scientific output of upcoming missions.

43 **1 Plain Language Summary**

44 Europa is a prime target in the search for life beyond Earth due to its global sub-
 45 surface ocean beneath an icy crust. Two major missions, JUICE and Europa Clipper,
 46 are set to arrive around 2030–2031 to investigate Europa's habitability. Plumes erupt-
 47 ing from the surface and carrying ocean material into space are among Europa's most
 48 intriguing features.

49 If these plumes leave surface deposits, they could offer an indirect way to detect
 50 activity. A plume was seen by the Hubble Space Telescope in 2012, but no further di-
 51 rect detections have followed. One method of identifying activity is by looking for sur-
 52 face changes over time. However, none have been observed, suggesting plume activity
 53 may be rare or absent.

54 Our study investigates another hypothesis. We model how long deposits from plume
 55 eruptions would last on Europa's surface, focusing on erosion caused by radiolysis and
 56 ion sputtering, the two most effective surface erosion processes.

57 We find that plume deposits erode quickly, geologically speaking, and their survival
 58 depends on location. These results suggest plumes could be active, but their surface sig-
 59 natures vanish too fast to observe. Our findings help future missions decide where to look
 60 and how soon after an eruption deposits must be observed.

61 **2 Introduction**

62 Europa, the fourth largest moon of Jupiter, is thought to harbour a subsurface wa-
 63 ter ocean beneath its icy crust, an environment that could potentially sustain life. This
 64 makes Europa one of the most compelling targets in the search for habitability beyond
 65 Earth (e.g. Chyba and Phillips (2002); Hand et al. (2009)). Multiple observations have
 66 suggested the presence of water vapour plumes erupting from its surface, possibly trans-

porting material from the ocean or subsurface water pockets to the surface. These plume could offer a rare opportunity to investigate the ocean's chemical composition (e.g. Lesage et al. (2025); Yoffe et al. (2025); Dayton-Oxland et al. (2023); Winterhalder and Huybrighs (2022); Huybrighs et al. (2017)). The value of directly sampling and analysing plume material was clearly demonstrated by Cassini's observations at Enceladus, where in-situ mass spectrometry of gases and dust particles detected salts (Postberg et al., 2009), organics (Khawaja et al., 2019), and geothermal activity (Waite et al., 2017). This underscores the potential of similar studies at Europa if active plumes can be identified and targeted by future missions.

Tentative evidence for plumes has been obtained from in-situ data and remote sensing observations. The Hubble Space Telescope (HST) detected the first potential water plumes at Europa's south pole over a seven-hour observation period in December 2012 (Roth et al., 2014). Furthermore, Galileo magnetic and plasma wave data has been interpreted as indirect evidence of plumes. Jia et al. (2018) reported an increase in plasma density, accompanied by a local decrease in magnetic field strength and field rotation, suggesting interaction with a plume. Similarly, Arnold et al. (2019) identified magnetic field perturbations in Galileo data consistent with a possible plume on Europa's trailing hemisphere. Several geological features have been identified as potential plume deposits, providing evidence for plumes in Europa's geological past. Lineated fractures, low albedo structures and other geological features on Europa's surface have been interpreted as cryovolcanic plume deposits which could highlight regions of recent geological activity and possible plume sources (Becker et al., 2023; Lesage et al., 2021; Steinbrügge et al., 2020; Quick et al., 2017; Fagents, 2003; Phillips et al., 2000; Fagents et al., 2000).

Observations in the same location as the 2012 HST observation in 1999, 2012 and 2015 (Roth et al., 2017, 2014) did not reveal any active eruptions, indicating that plume activity may be intermittent. This is further supported by Paganini et al. (2020), where only one out of 17 observations from February 2016 to May 2017 indicated a potential plume detection. Moreover, Kimura et al. (2024) failed to detect any plume-related water vapour signatures using high resolution infrared spectroscopy. Similarly, Hansen et al. (2024) and Villanueva et al. (2023) did not detect any active eruptions or volatile emissions in their surveys using Juno and JWST, respectively.

The transient nature of Europa's plumes makes it essential to understand how long their deposits persist on the surface following an eruption. By investigating the lifetime of plume deposits, we improve our understanding of Europa's surface activity and provide constraints for estimating the exchange of material between the surface and the subsurface ocean. This information is also valuable for optimizing the observational strategies of upcoming missions such as Jupiter Icy Moons Explorer (JUICE) and Europa Clipper. These missions aim to investigate Europa's surface and subsurface properties using high-resolution imaging, spectroscopy, and in situ plasma, neutrals and magnetic fields measurements, with the goal of assessing the moon's habitability and searching for signs of recent or ongoing activity (Masters et al., 2025; Tosi et al., 2024; Pappalardo et al., 2024). The detection of a plume's deposit would provide the best evidence of recent plume or geological activity on Europa and could also serve as an important indicator for where to search for ongoing activity.

As previously mentioned, it has been hypothesized that particles released from Europa's interior are deposited onto its surface. Theoretically, deposited particles could leave a detectable trail on the surface. Optical observations have so far failed to detect any conclusive changes on Europa's surface during the recent observation epoch enabled by missions to Europa (Hansen et al., 2024; Schenk, 2020). Specifically, Schenk (2020), presented three 50 km resolution global imaging maps of the surface obtained in 1979, 1996–1998, and 2007 by Voyager, Galileo, and New Horizons, respectively, and searched for surface changes related to plume deposits. These maps revealed no obvious albedo, colour patterns or surface changes related to plume activity that could be identified with confidence

120 on the surface over the ~ 28 year period. Due to the limited resolution of the observation
 121 (approximately 50 km), any potential surface changes smaller than this value could
 122 not have been detected, if they occurred.

123 In this work, we investigate the hypothesis that plume deposits are subject to ex-
 124 ternal erosion factors and therefore may have a short lifespan. This idea is consistent with
 125 previous suggestions that deposits from plume activity might erode quickly due to the
 126 bombardment of Europa's surface by charged particles (Tseng et al., 2025; Phillips et
 127 al., 2000). In particular, Tseng et al. (2025) argued that even if plume activity occurred
 128 in the past, the lack of visible surface signatures in Schenk's long-term imaging compar-
 129 ison could be explained by the rapid erosion or modification of the deposited material
 130 by erosion due to impacting charged particles.

131 In this study, we take a broad approach by analysing how different types of plume
 132 activity (mass flux, eruption time) and the locations of the plumes could influence the
 133 longevity and detectability of their surface deposits. Two key processes that we consider
 134 are ion sputtering and radiolysis, both of which have been extensively studied in the past
 135 (e.g. Addison et al. (2022, 2021); Vorburger and Wurz (2018); Plainaki et al. (2018); Galli
 136 et al. (2018); Cassidy et al. (2013); Plainaki et al. (2012)).

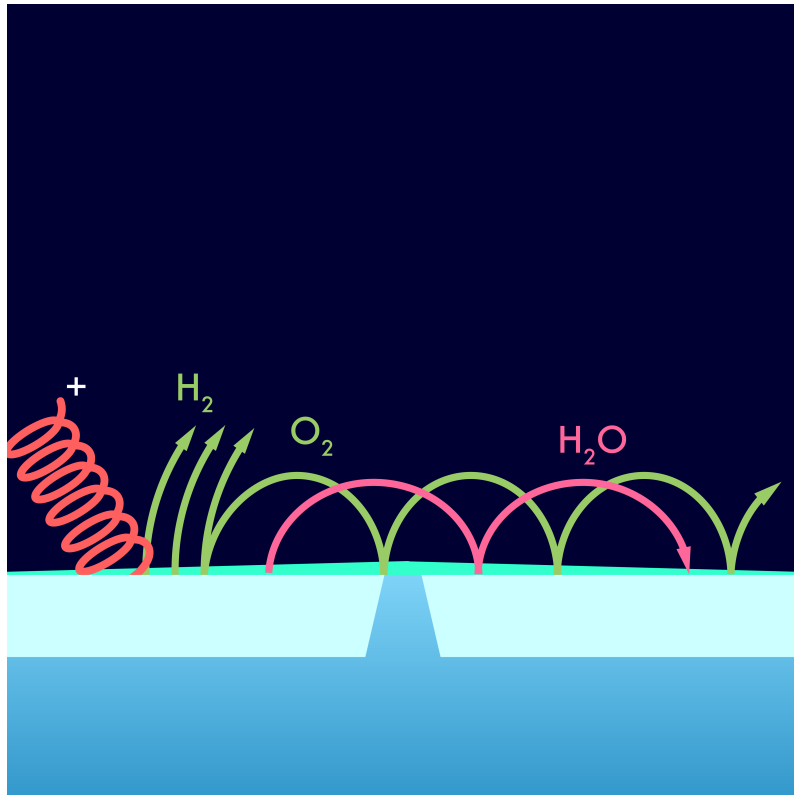


Figure 1: Schematic illustration of erosion processes acting on a plume deposit. The cyan surface represents the deposited plume material, which is impacted by incoming energetic ion (red helix). This interaction initiates two key processes: ion sputtering and radiolysis. Sputtered H_2O (pink arc) bounces away and eventually stick to the surface. Radiolysis produces H_2 , and O_2 , which are then sputtered. H_2 escapes the surface, while O_2 continues migrating across the surface, potentially reaching the poles and sticking there. Please note that the relative size of the particle trajectories and surface layers in this schematic are not intentional.

Figure 1 shows a schematic overview of the sputtering and radiolysis processes. Energetic ions (and energetic electrons) impacting the surface of Europa can either sputter the water ice molecules or excite them or ionize them. Following electronic excitations and ionizations water molecules are dissociated (radiolysis) producing predominantly H and OH with a much smaller fraction of H₂ and O, possibly only occurring at surfaces, grain boundaries and voids (Watanabe et al., 2000). At the temperatures on Europa, H diffuses until it reacts, whereas the OH and O trap (R. E. Johnson, 2001). As temperature increases these radicals are mobilized (Matich et al., 1993) possibly producing oxygen, water and/or additional new molecules (Kimmel et al., 1994; Orlando & Kimmel, 1997) such as H₂O₂ and HO₂. The newly formed molecules are then ejected from the surface to the moon's exosphere. Assuming this pathway, we suggest that neutral water molecules deposited on Europa's surface after plume eruptions interact with the energetic ions bombarding it, a process that predominantly leads to the release of water, oxygen, and hydrogen molecules to the exosphere (Plainaki et al., 2010; R. Johnson et al., 2009). Upon bombardment, sputtered water molecules return to the surface of Europa. Teolis et al. (2017a) described that water molecules returning to the surface first stick, then either thermally desorb at the local surface temperature, re-sputter back into the exosphere, or diffuse into the porous regolith. However, the most erosive factor is radiolysis, which consists of the decomposition of the deposited water molecules due to ionising radiation, eventually resulting in the production of molecular oxygen (O₂), and molecular hydrogen (H₂) (Szalay et al., 2024; Plainaki et al., 2010). After the decomposition of the water molecules, the light H₂ molecules escape Europa's gravitational pull and dissipate in space, while O₂ undergoes a more complex journey (see Figure 1).

Most of the O₂ released from the surface (approximately 98%) does not escape gravity. In Plainaki et al. (2012), the authors assumed that the O₂ that re-impacts the surface never sticks on it but bounces back and forth, getting thermalised at each impact, until it is finally lost, predominantly through ionization. More recently Teolis et al. (2017a) have shown that oxygen could stick to Europa's surface when reaching the poles, where Europa's surface temperature drops significantly.

The main objective of this study is to determine the order of magnitude of the erosion timescale for deposited plume material. We investigate how long a plume deposit can persist on Europa's surface as a function of its mass flux and eruption time, thereby offering valuable insight into the lack of observed surface changes reported by Schenk (2020). We present a first order estimate of the erosion timescale of plume deposits by simulating the rate at which such material is removed under two scenarios, (a): very close (10 km) to the plume source which we will refer to as Model 1, and (b): just outside the resolution limit of Schenk (2020), which we will refer to as Model 2; across various durations of plume activity and mass flux.

Estimating how quickly deposited particles are eroded by sputtering and radiolytic processes, under various plume characteristics, enhances our understanding of Europa's surface-exosphere interactions. Moreover, these results could inform the targeting strategies of JUICE and Europa Clipper missions aiming to study active plumes and their associated surface deposits directly.

3 Methodology

In order to investigate the erosion time of plume deposits on Europa under varying conditions (plume mass flux, plume eruption time and localised erosion rates), we developed two scientific models. The two models investigate, respectively, the time it takes to erode a plume deposit that is confined to a 10×10 km area near the plume source, and the time it takes for a plume deposit to shrink to an area smaller than 50×50 km size (the observational limit from Schenk (2020)).

187 Both models rely on the same plume setup and on similar baseline assumptions.
188 We based our plume characteristics on the HST plume detection in December 2012, where
189 this plume was observed for 7 hours and had a mass flux of 7,000 kg/s (Roth et al., 2014).
190 In our study, we vary the following two key plume parameters: mass flux and eruption
191 time, as these parameters remain poorly constrained due to limited and tentative na-
192 ture of the current observations. We considered a wide range of mass flux values, from
193 1 kg/s to 10,000 kg/s. Different types of plumes might exist, but observations are very
194 limited, and especially low mass flux plumes might not be detected using current tech-
195 niques (Huybrighs et al., 2017). Similarly, a broad range of eruption durations was ex-
196 plored, from a few seconds to up to one year, since the true duration of observed or hy-
197 pothetical plumes remains uncertain.

198 The plume models employed in this work are based on the modelling approach from
199 Huybrighs et al. (2017) and Winterhalder and Huybrighs (2022), where the authors per-
200 formed a non collisional, Monte Carlo simulation of several plume candidates and eval-
201 uated the feasibility of detecting them during planned flybys by JUICE. These models
202 assume a collisionless distribution of neutral H₂O molecules emitted symmetrically from
203 a point-source plume. The initial conditions of the molecules are determined by a Maxwellian
204 velocity distribution corresponding to a gas temperature of 230 K and an imposed av-
205 erage outflow velocity of 460 m/s perpendicular to the surface. As shown in Figure 2,
206 the resulting particle density above the surface follows a spatial distribution that peaks
207 near the source and diminishes with increasing distance. According to Huybrighs et al.
208 (2017), these H₂O molecules follow ballistic trajectories under Europa's gravity and most
209 of them ultimately re-impact the surface, forming a localised deposit layer. We assume
210 that this fresh deposit layer has different optical properties from Europa's complex and
211 inhomogeneous surface, making the deposit detectable. In our model we assume no losses
212 of H₂O due to processes such as electron impact ionization (Huybrighs et al., 2017) oc-
213 cur before they reach the surface.

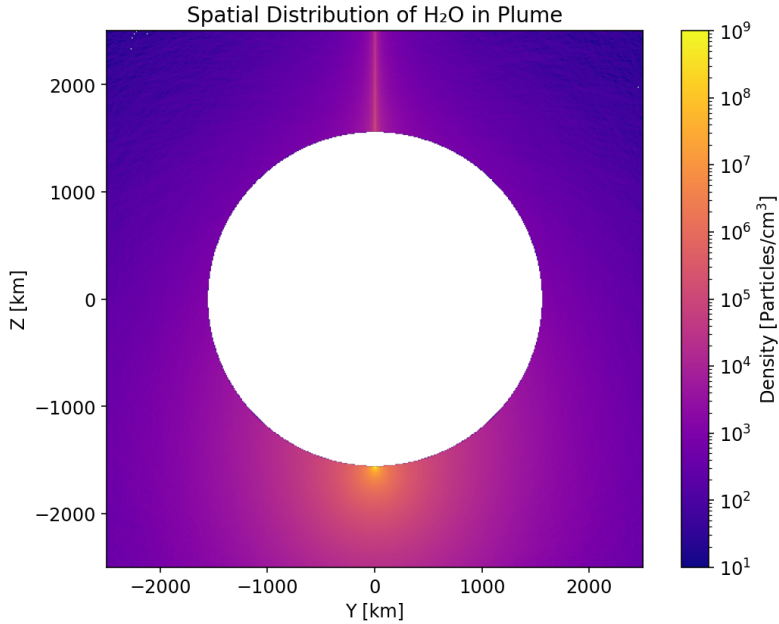


Figure 2: Spatial distribution of H_2O neutral density around Europa resulting from a plume source at the south pole, with a source mass flux of 7,000 kg/s. The reference frame used in this work is the IAU Europa-centered reference frame Archinal et al. (2011): the z -axis is perpendicular to Europa's mean orbital plane (pointing north), the x -axis points from Europa toward Jupiter, and the y -axis completes the right-handed system (opposite to Europa's orbital motion and the direction of the corotational plasma flow).

Over time, the deposit erodes as a result of the erosion mechanisms previously outlined in the introduction, exposing the original terrain underneath the deposit. The values for the erosion factors of radiolysis and ion sputtering adopted in this work are taken directly from Plainaki et al. (2012). The qualitative estimates for these erosion factors, such as radiolysis and sputtering, vary by one to two orders of magnitude across the literature (Szalay et al., 2024; Addison et al., 2022; Teolis et al., 2017a, 2017b; Cassidy et al., 2013). Consequently, our calculated erosion times may also vary within a similar range. However, this level of variation does not significantly impact the broader conclusions that plume deposits are short lived compared to Europa's surface age for a wide range of plume eruption times and mass fluxes.

A notable assumption within the radiolysis process concerns the fate of O_2 molecules produced on Europa's surface. After formation, these molecules are sputtered from the surface by incoming energetic ions. As previously mentioned (see Section 2), some studies assume that O_2 does not stick on the surface, while others have shown a temperature dependence for O_2 sticking. In our work we generally assume that the O_2 does not stick after erosion. We will also discuss the erosion time in the special case of Europa's colder poles. Furthermore, in both our models we assume that neither sputtered H_2O nor O_2 return to the same spatial region from which they were ejected. In our study, we consider a localized simulation domain of 10×10 km. For sputtered O_2 or H_2O molecules to fall back within this domain, they would need to be ejected with energies as low as 10^{-3} eV. This is well below the average ejection energy of sputtered O_2 and H_2 (Plainaki et al., 2012), making the fallback into the same domain as they originated from highly unlikely.

Location dependence of the erosion factors (original units and converted to $\text{kg}/\text{m}^2 \cdot \text{s}$)

Location	Sputtering Rate		Radiolysis of O_2		Radiolysis of H_2	
	$\text{H}_2\text{O}/\text{m}^2 \cdot \text{s}$	$\text{kg}/\text{m}^2 \cdot \text{s}$	$\text{O}_2/\text{m}^2 \cdot \text{s}$	$\text{kg}/\text{m}^2 \cdot \text{s}$	$\text{H}_2/\text{m}^2 \cdot \text{s}$	$\text{kg}/\text{m}^2 \cdot \text{s}$
Maximum	2.251×10^{15}	6.73×10^{-8}	2.714×10^{16}	1.44×10^{-9}	6.23×10^{14}	2.09×10^{-13}
Minimum (equator)	3.621×10^{14}	1.08×10^{-8}	1.19×10^{16}	6.30×10^{-10}	1.498×10^{14}	5.01×10^{-13}
Average	2.5×10^{14}	7.48×10^{-9}	6.3×10^{13}	3.33×10^{-9}	8×10^{13}	2.79×10^{-11}

Table 1: This table presents the values used to implement Model 1 and 2, highlighting the variability of erosion factors across different locations on Europa. These values, specifically sourced from Table 1 and 2 in Plainaki et al. (2012), provide critical data on how sputtering and radiolysis rates change depending on the location on Europa's surface. The values for the maximum case for both radiolysis and sputtering are the sum of $f_{\text{sputtering}}$ at the trailing hemisphere apex (THAP) (Table 1) and f_{O_2} and f_{H_2} at small altitude above the subsolar point (SSP) (Table 2) for all the impacting ions. The fluxes for the erosion factors at the minimum case (poles) represent an estimate and were obtained by summing $f_{\text{sputtering}}$ at trailing hemisphere antapex (THAN) (Table 1) and f_{O_2} at the antisolar point (ASP) and f_{H_2} at small altitude above ASP (Table 2) for all impacting ions.

The described erosion factors are highly dependent on local temperatures and on ion fluxes that vary over the surface of Europa (e.g. Addison et al. (2022); Teolis et al. (2017a); Plainaki et al. (2012)). Based on the outlined geographic location in Plainaki et al. (2012), we consider three representative scenarios at the equator: maximum, minimum and average erosion cases. The maximum erosion case at the equator corresponds to the trailing hemisphere (T.H.) and subsolar point (S.P.) where sputtering is enhanced due to higher ion fluxes, and radiolysis is accelerated by high solar flux. In contrast, minimum equatorial erosion conditions were assigned to the leading hemisphere (L.H.) and polar regions or anti-solar point (A.P.), where reduced solar incidence decreases the rate of erosion processes. Studies of Europa's temperature suggest that the true minimum effect of radiolysis process might be at the poles of Europa. Here the temperature drops significantly, and so does the radiolysis yield, which we will discuss in Section 4.

Note that the fluxes reported by Plainaki et al. (2012) and summarised in Table 1 include both freshly sputtered ("newborn") molecules escaping the surface and previously released molecules that undergo multiple surface interactions (i.e., bouncing trajectories). Even if only the newborn component was considered, the resulting flux would be reduced by approximately a factor of two. However, given that the primary objective of this study is to estimate the order of magnitude of the erosion timescale, this level of uncertainty is acceptable, and the full flux values were used. The details of the computational methods and implementation details specific to each model are described in the following section.

Our study focuses specifically on the effects of radiolysis and ion sputtering on the removal of plume deposits as they are the main erosion processes. However, we have not considered other weaker loss processes and mechanisms that may also affect the particles. For instance, these plume deposits are released into space when impinged upon by UV photons, a process known as "photon-stimulated desorption" (Plainaki et al., 2012). This process might also provide some contribution to the atmospheric population, although estimations based on laboratory data show that this process, in general, is not the dominant one at Europa (Plainaki et al., 2012). Another erosion mechanism that is thought to be weaker are meteoric impacts which cause a modification of the surface (Szalay

et al., 2024). A detailed investigation of the role of these other processes is out of the scope of the current analysis.

269 3.1 Model 1: Confined Domain Within 10 km from the Source and Uni- 270 form Deposition of Particles

In this model, we investigate the erosion timescale of a hypothetical case in which all plume material is deposited on a 10×10 km area centred on the plume source. We treat this as a closed system: all particles ejected from the plume are assumed to deposit uniformly within this volume, and no mass exchange occurs with the surrounding environment. The motivation behind this case is to evaluate whether plume deposits could

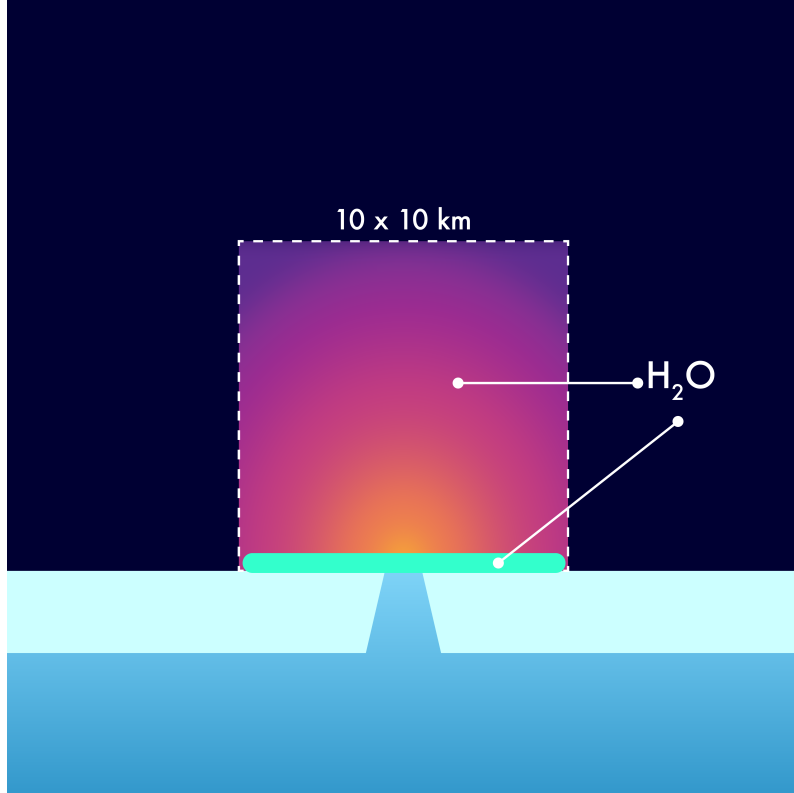


Figure 3: Schematic illustration of the spatial setup used in Model 1, showing the 10 km region centred on the plume source where all particles are assumed to deposit uniformly (no particle dispersion), thereby forming a deposit represented by the blue thick band.

be eroded over geologically short timescales even if all ejected and deposited material is confined to a small region compared to the size of Europa. Under this assumption, the mass flux of deposited material is used to determine the mass of particles falling onto the surface. In this closed system, the mass flux of ejected particles (\dot{m}) integrated over time equals the mass of deposited particles (M). The mass of deposited particles is calculated using the following equation where t_e refers to the eruption time of the plume:

$$M = \dot{m} \cdot t_e \quad (1)$$

271 Model 1 provides an upper-limit estimate for the lifetime of the deposit, as this the-
272 oretical study focuses on the deposit near the source and assumes uniform deposition.

To do so, we consider the combined effect of dominant erosion mechanisms, collectively represented as the erosion rate (r_e). These include the average sputtering rate of water molecules (s_R) and the average radiolysis of both O_2 and H_2 , as described in Plainaki et al. (2012) and summarized in Table 1. To determine the disappearance time of the deposit, we solve for the time when all deposited particles have been eroded from the surface (equation 2). This yields the maximum erosion time T_{max} (equation 3). The parameter A denotes the surface area over which particles are deposited, taken to be the face of a cube with side length 10 km. This spatial scale is approximately consistent with observational constraints, as candidate plume deposits on Europa have been identified on scales of several kilometres (e.g. Quick et al. (2022); Phillips et al. (2000)).

$$M - r_e \cdot A \cdot T_{max} = 0 \quad (2)$$

$$T_{max} = \frac{M}{r_e \cdot A} \quad (3)$$

283

3.2 Model 2: Expanded Domain Outside 50 km Observational Limit and Non-Uniform Particle Deposition informed by Plume Model

While Model 1 provides valuable insights into the erosion timescales of very confined plume deposits near the source, it cannot be directly compared with the results of Schenk (2020). This is due to two factors: (a) Model 1 focuses on a 10 km cubic volume, which lies well within the 50×50 km observational constraint outlined by Schenk (2020), and (b) it assumes a closed system in which all ejected particles fall back into the same region, neglecting the spatial dispersion of the ejected material (see Figure 2) which has been modelled by studies such as Tseng et al. (2025); Dayton-Oxland et al. (2023); Winterhalder and Huybrighs (2022); Vorburger and Wurz (2021); Huybrighs et al. (2017); Berg et al. (2016).

To better assess the longevity of plume deposits at larger distances from the source and to establish a meaningful comparison with the observational limitations presented in Schenk (2020), we introduce a second model. Here, we evaluate the erosion time of particles that land 25 km away from the plume source. This location lies just outside the observational limit of 50 km and provides a representative case for exploring the fate of particles at the outer edge of the detectable region (Figure 4). By focusing on this specific distance, rather than simulating the entire spatial domain, we aim to determine the maximum time available for plume deposits to remain observable before retreating into regions smaller than the observational limit from Schenk (2020) (50 km).

304

In this model, the density distribution of particles ejected by the plume is explicitly considered using the plume model outputs from Winterhalder and Huybrighs (2022) and Huybrighs et al. (2017). Unlike Model 1, where the mass flux towards the surface was assumed uniform across the region, in Model 2 the mass flux towards the surface varies with distance from the source. This is due to the spatial distribution of the ejected collisionless particles: the density is highest directly above the plume and decreases with distance. This approach then allows us to extend the model to account for infalling mass flux in the new location.

313

However, while the particle density is spatially resolved, the velocity of the particles impacting the surface is treated as constant. In reality, plume particles impacting the surface exhibit an increase in velocity as they move farther from the source as they represent the tails of the velocity in a Gaussian distribution (Huybrighs et al., 2017). However, this velocity gradient only becomes significant at much larger distances. Because

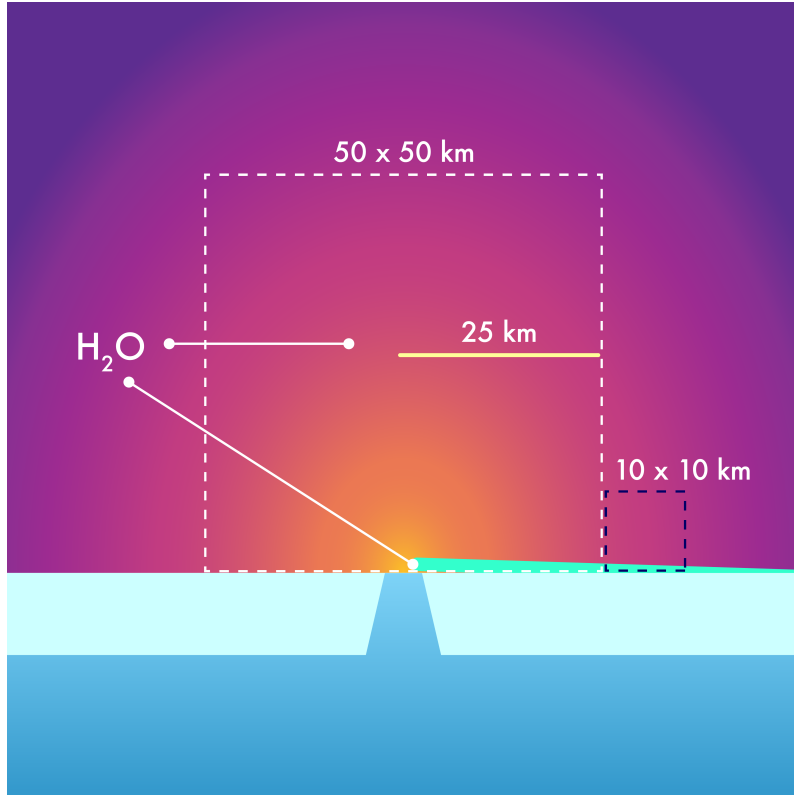


Figure 4: Diagram showing the geometry used in Model 2, where we estimate the erosion time of particles deposited (cyan sloped line) at a distance of 25 km from the plume source, just outside the 50×50 km observational limit in Schenk (2020).

we are only seeking a first order approximation and our focus remains within 25 km of the source, we neglect this effect and adopt a constant average velocity (460 m/s), as given by Huybrighs et al. (2017). This value overestimates the actual particle velocities at 25 km from the source. Assuming a uniform ejection angle and an average velocity of 460 m/s, the majority of particles travel distances exceeding ~ 50 km. Therefore, using this constant velocity leads to an overestimation in impact speed at 25 km, and consequently, an overestimation of the erosion timescale.

An important assumption in Model 2 is that all deposited water particles adhere perfectly to the surface upon impact, forming a uniform layer that entirely covers the underlying terrain. This assumption maximises the retention efficiency of the deposited material and, as such, provides an upper limit for the longevity of the deposit. It is important to note that in reality H_2O molecules ejected by the plume or sputtered by incident ions may bounce before sticking to the surface. The perfect adherence assumption simplifies the mass budget and facilitates the derivation of an upper-bound estimate for erosion timescales, but should be revisited in future models incorporating more detailed surface physics. To calculate the mass flux of falling particles at the 25 km mark, we used the density distribution derived from the plume simulations of Winterhalder and Huybrighs (2022) at this distance, which are publicly available in Casado-Anarte and Huybrighs (2025). The infalling mass flux at this point, denoted as \dot{m}_f , is computed via

$$\dot{m}_f = n_{25 \text{ km}} \cdot v_{avg} \cdot A \quad (4)$$

325 where $n_{25 \text{ km}} = 4.71 \times 10^6 \text{ particles/cm}^3$ is the number density at 25 km from the plume
 326 source for a plume with a mass flux of 1 kg/s, v_{avg} is the constant average particle ve-
 327 locity (460 m/s), and A is the effective cross-sectional area of the landing region. Once
 328 the mass flux at 25 km is determined, equations [1],[2] and [3] are used to determine T_{max}
 329 at 25 km from the plume source. As the density of the plume in the non-collisional model
 330 of Huybrighs et al. (2017) and Winterhalder and Huybrighs (2022) scales linearly with
 331 the plume's mass flux, we can evaluate plumes of different mass fluxes by linearly scal-
 332 ing Equation 4.

333 Model 2 investigates how spatial variations in Europa's surface environment influ-
 334 ence the erosion of plume deposits. Radiolytic erosion is primarily dependent on local
 335 surface temperature, while ion sputtering varies with the flux and energy of incident Jo-
 336 vian plasma ions. To capture these effects, two sets of simulations were performed us-
 337 ing the values listed in Table 1. First, the individual contributions of sputtering and ra-
 338 diolysis were assessed independently by applying equatorial minimum, average, and max-
 339 imum erosion rates to a deposit located 25 km from the plume source. This approach
 340 isolates the influence of each mechanism under varying environmental conditions. Sec-
 341 ond, the combined effect of both sputtering and radiolysis mechanisms was evaluated for
 342 representative surface regions corresponding to equatorial minimum, average, and max-
 343 imum erosion scenarios. All cases assume static environmental conditions for simplic-
 344 ity. However, given Europa's 3.5 day orbital period around Jupiter, surface conditions,
 345 particularly ion flux and temperature, vary significantly over time. A more comprehen-
 346 sive treatment would require modeling the time-dependent exposure of the deposit to
 347 changing irradiation conditions as Europa moves through Jupiter's magnetosphere.

348 4 Results and Discussion

349 To assess the lifetime of surface deposits formed by Europa's plume activity, we in-
 350 vestigated the erosion timescale of deposited material as a function of eruption duration
 351 and mass flux. The analysis, carried out under variation of the surface temperature and
 352 impacting ion fluxes representative of Europa, demonstrates a clear limitation on plume
 353 deposit lifetime due to erosion by radiolysis and sputtering.

354 4.1 Model 1 Suggests Plume Deposits Likely Eroded Before Recent Imag- 355 ing Epochs

356 Figure 5 shows the dependence of the erosion time as a function of plume mass flux
 357 and eruption time for Model 1. In the figure, the white contour line marks an erosion
 358 time of 28 years, a threshold chosen to represent the temporal separation of the obser-
 359 vations in Schenk (2020). Plume eruptions characterized by parameters falling below this
 360 white contour line result in deposits that are eroded within 28 years due to sputtering
 361 and radiolysis.

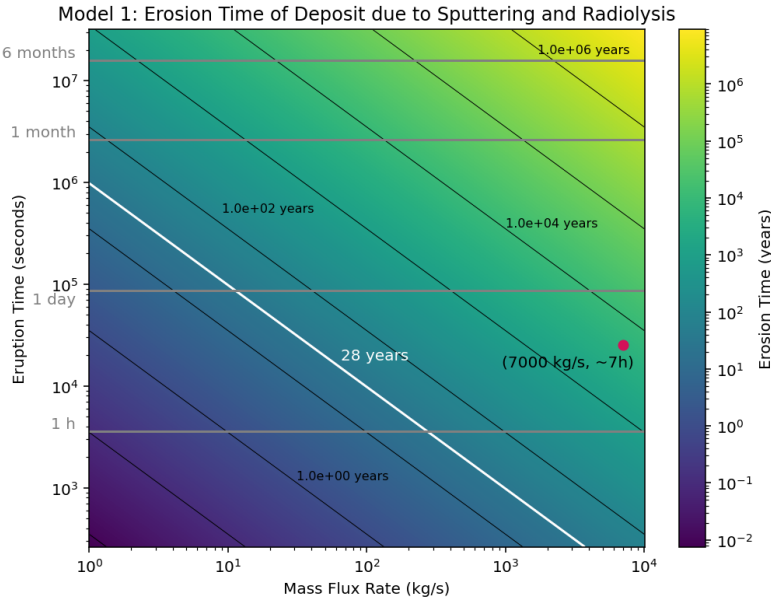


Figure 5: Erosion time of the plume’s deposit as a function of mass flux and time of eruption for Model 1. The magenta dot represents the plume observed by HST in 2012 (a 7,000 kg/s plume active for 7 hours).

Figure 5 shows that the lifetime of a plume deposit in Model 1 is strongly limited by the two erosion parameters. Notably, the estimated erosion time for the plume observed by HST, which released 1.76×10^8 kg of particles, falls beyond the 28 year limit, with a predicted erosion time of approximately 5050 years in this hypothetical scenario, which is very short compared to the estimated 60 Ma age of Europa’s surface (Bierhaus et al., 2009; Schenk et al., 2004; Zahnle et al., 2003). This implies that, even when looking at a closed system in which all released plume particles are confined to a 10×10 km surface area and using averaged values for the erosion factors, plume deposits are geologically short lived. Therefore this model highlights the importance of further investigating the erosion of deposits with plume models that account for a physically realistic spatial distribution of the deposit.

In addition, Model 1 suggests plume deposits likely eroded before recent imaging epochs. Therefore the lack of observational evidence for large plume deposits (of scale of tens to hundreds km size) does not necessarily mean there is no plume activity on Europa. In fact, if a plume were to erupt repeatedly on timescales shorter than the erosion lifetime, its deposit would persist and be detectable in current observations. The absence of such deposits therefore supports the idea that eruptions are infrequent or singular. One proposed explanation for the lack of repeated activity is vent sealing (Boccelli et al., 2025). This reinforces the conclusion that, even under idealized assumptions, plume deposits are geologically short-lived and would not be expected to remain visible on Europa’s surface today.

4.2 Model 2 Suggests Plume Deposits Shrink Below Observable Scales

While Model 1 provides a valuable first-order estimate of deposit survival and illustrates the broad sensitivity of erosion timescales to eruption parameters, it is not directly comparable to the observations reported by Schenk (2020) because Model 1 lies within the observational constraints. To address this limitation and provide a more re-

388 realistic representation of a plume event, Model 2 focuses on investigating how long it takes
 389 for plume material to erode outside the 50×50 km area around the source. To do so
 390 we investigate the erosion at a location 25 km away from the source. Additionally, this
 391 model incorporates a physically informed particle distribution for the ejected material,
 392 offering a more accurate depiction of the deposition profile. As such, Model 2 yields re-
 393 sults that are more consistent with expected conditions on Europa and more directly com-
 394 parable to observational data.

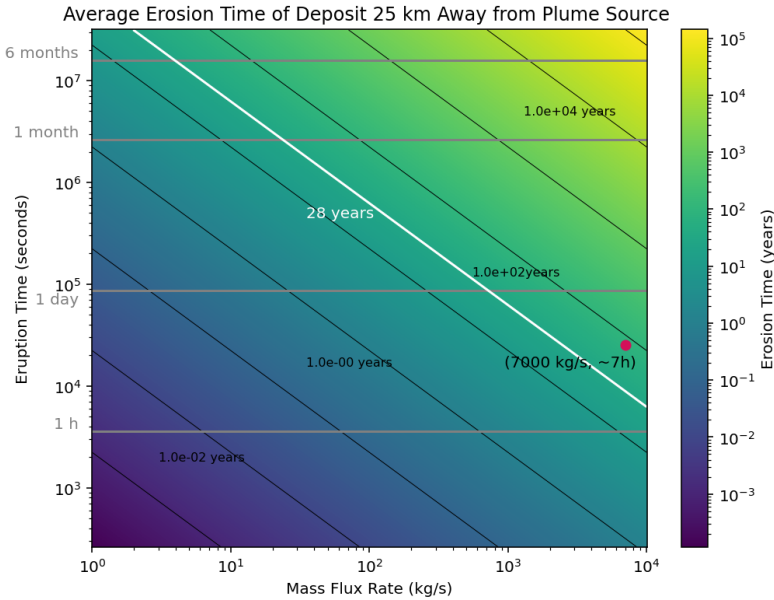


Figure 6: Erosion time of plume's deposit as a function of mass flux and time of eruption 25 km away from the source. The magenta dot represents the plume observed by HST in 2012 (a 7,000 kg/s plume active for 7 hours)

395 Figure 6 presents the estimated erosion timescale for a deposit at 25 km from the
 396 source, using average values for sputtering and radiolysis rates (see Table 1). Model 2
 397 indicates that erosion progresses more rapidly at increasing distances from the plume source.
 398 This trend arises from the decreasing number of deposited material with distance, as fewer
 399 particles reach farther regions, resulting in thinner layers. As a result, deposits located
 400 at greater distances not only erode more quickly, but are also less likely to persist to be
 401 detected across typical observational timescales.

402 The results from Figure 6 suggest a deposit outside of the 50×50 km area cen-
 403 tered at the source has a lifetime of approximately 33 years for the HST-detected plume.
 404 These findings allow for an alternative interpretation of the results presented by Schenk
 405 (2020), where they found no observable changes on the surface of Europa. For plumes
 406 whose deposits fall below the 28-year erosion threshold illustrated in Figures 5 and 6,
 407 it is likely that surface features would have eroded before becoming detectable beyond
 408 the 50 km observational range employed in that study. Our findings suggest that a plume
 409 erupting at the beginning of a 28-year period could have its deposits completely eroded
 410 25 km away from the source by the end of that interval, and therefore would no longer
 411 be visible within the observational constraints of the image data used in that study.

412 It is worth noting that Schenk (2020) primarily searched for large-scale, long-lived
 413 deposits. Based on the upper limits of our models, i.e., a hypothetical plume active for

414 a year with a mass flux of 10,000 kg/s, we estimate that any resulting deposits outside
 415 the 25 km distance from the source would persist for only \sim 10 Ma. We emphasize that
 416 such extreme cases exceed observational constraints of the HST-plume. Even for these
 417 extreme plumes the estimated lifetime is significantly shorter than Europa's average sur-
 418 face age of \sim 60 Ma (Schenk et al., 2004; Zahnle et al., 2003; Bierhaus et al., 2009). This
 419 suggests that plume-related features, even if initially substantial, are unlikely to persist
 420 at scales larger than 50 km over geological timescales and may have been entirely removed
 421 by continuous erosion processes.

422 The types of plumes detected by HST might be rare exceptions, with smaller plumes
 423 (in size) possibly being more common (Quick & Hedman, 2020). Quick et al. (2022) in-
 424 vestigates small-scale (less than 10 km) deposits from ice-rich plumes. We propose a hy-
 425 pothesis that such deposits may have originated from larger plumes, in which the ma-
 426 jority of the area covered by the plume deposit has since been eroded. The deposits in-
 427 vestigated in Quick et al. (2022) could thus be leftovers of initially much larger deposits
 428 and spatially larger plumes. In the case of much smaller plumes, the observed deposits
 429 would require most of the ejected material to settle near the source region, consistent
 430 with the behaviour described in Model 1 (Section 4.2). Note that lifetimes could exceed
 431 those from Model 1 if plume deposits were even more confined than 10 by 10 km.

432 In addition to explaining the absence of detectable deposits, our model also offers
 433 a means to constrain plume characteristics in cases where deposits are observed and their
 434 size changes over time. If future missions were to re-image a candidate deposit and de-
 435 tect shrinkage, for instance, a retreat of 10 km over 10 years, this erosion rate could be
 436 compared to the erosion rates predicted in our models. This would enable us to estimate
 437 which combinations of plume mass flux, eruption duration, and local erosion conditions
 438 are consistent with the observed evolution. Conversely, if a deposit remains unchanged
 439 across repeated observations, it implies that the local erosion rate is lower than the rate
 440 required to remove the deposit over that time, placing a lower bound on either the age
 441 or mass of the deposit. In both cases, observational data can be used to refine or invert
 442 the model to extract physical properties of the source event.

443 4.3 Plume Deposit Erosion Strongly Depends on Location

444 While the previous section considered the average combined effect of sputtering and
 445 radiolysis on a deposit located 25 km from the plume source, here we examine each ero-
 446 sion factor independently and in location-specific contexts. This decomposition is essen-
 447 tial for understanding how plume deposit longevity varies across Europa's surface, where
 448 the variation of ion fluxes and surface temperature affects erosion timescales. Such an
 449 approach also allows for the identification of surface regions where deposits may survive
 450 longer or erode more rapidly, contributing to the interpretation of observational constraints
 451 and the understanding of the effect of these factors on plume deposits.

452 Figure 7 presents the influence of the individual erosion processes, ion sputtering
 453 and radiolysis, applied to a plume deposit located 25 km from the source (Model 2). Each
 454 process is evaluated using minimum and maximum rates (see Table 1), across four rep-
 455 resentative locations: sputtering at the Trailing and Leading hemispheres (panels a and
 456 b), and radiolysis at the Subsolar and Antisolar points (panels c and d).

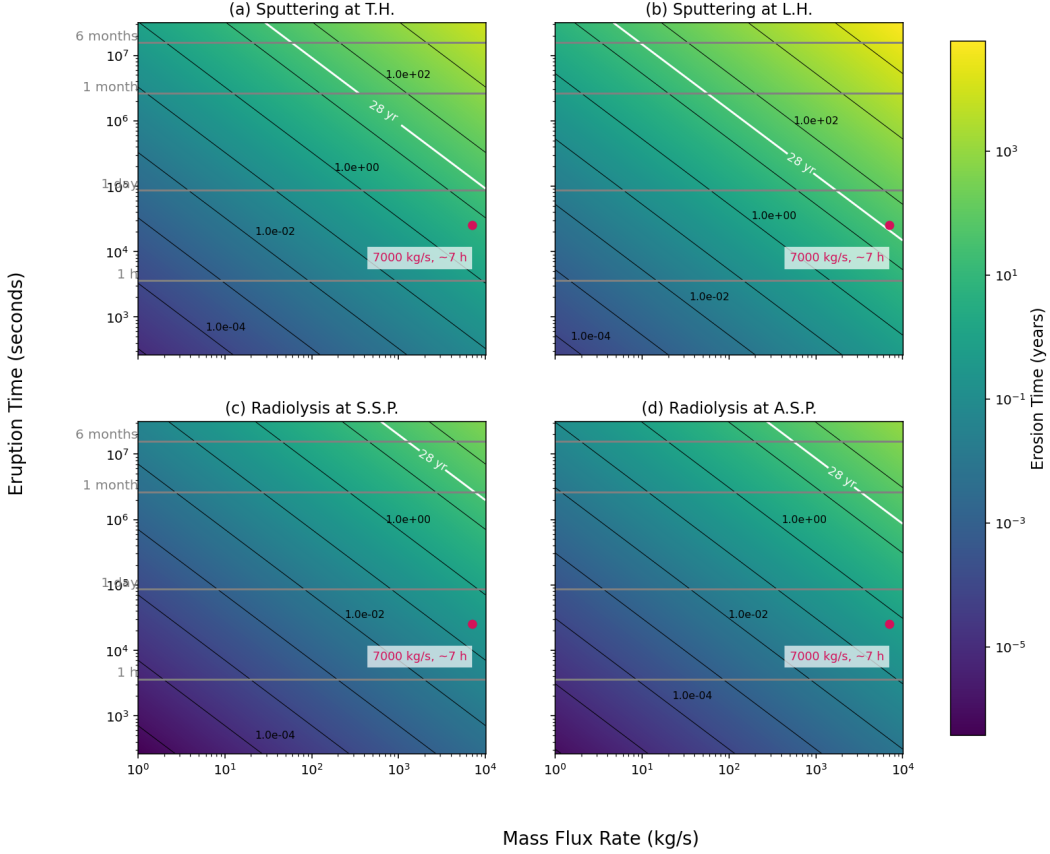


Figure 7: Erosion time of a plume deposit located 25 km away from the source, evaluated under varying plume mass flux and eruption durations. Each panel isolates the effect of a single erosion factor, either ion sputtering or radiolysis, under specific surface conditions representative of different regions on Europa. Panels (a) and (b) show sputtering erosion at the trailing (T.H.) and leading hemispheres (L.H.), respectively. Panels (c) and (d) display radiolysis driven erosion at the subsolar (S.S.P.) and antisolar (A.S.P.) points.

457 Although the ion sputtering rate we use is less than the radiolysis rate (see Table
 458 1), the upper bound results shown in panels (a) and (b), which correspond to sputtering-
 459 only scenarios, demonstrate that for a plume of 10,000 kg/s active over one year, a de-
 460 posit located 25 km from the source could survive for tens of thousands years. This is
 461 consistent with our previous discussion regarding the short lifetime of plume deposits.
 462 In the specific case of the plume observed by HST (7,000 kg/s active for 7 hours), the
 463 estimated erosion time is approximately 5 years if the deposit resides on the Trailing hemi-
 464 sphere (panel a), and ~ 33 years on the Leading hemisphere (panel b), showing that lo-
 465 cation influences sputtering efficiency by roughly an order of magnitude.

466 Radiolysis, by contrast, emerges as a much more dominant erosion mechanism. Pan-
 467 els (c) and (d) of Figure 7 show that under both Subsolar and Antisolar conditions, de-
 468 posits located 25 km away from the source are eroded in less than a year for a HST-plume
 469 type. However, for the most intensive plume in our model, the erosion time differs by
 470 an order of magnitude. The temperatures at these equatorial locations are never as cold
 471 as near the poles, where the radiolysis effect would notably decrease. This result may
 472 prove particularly useful for future studies investigating erosion at polar latitudes, where
 473 lower surface temperatures are expected to significantly enhance the longevity of plume

474 deposits. For reference, Europa's polar temperatures are around 40 K, compared to approximately 80 K at the antisolar point (Teolis et al., 2017a). Based on Plainaki et al.
 475 (2012), the yield of O₂ production via radiolysis can be estimated at these temperatures
 476 using their equations (2) and (3) from their study, which are based on (Famá et al., 2008).
 477 Their analysis shows that the efficiency of O₂ production by S⁺ ion impact decreases by
 478 roughly two orders of magnitude between 80 K and 40 K (see Figure 1 in Plainaki et al.
 479 (2012)). Hence, a conservative approximation suggests that O₂ production, and by ex-
 480 tension surface erosion due to radiolysis at the poles, even in the absence of precise quan-
 481 titative models for radiolysis at this location, would be two orders of magnitude lower
 482 than at the antisolar point. Consequently, this strongly supports the idea that plume de-
 483 posits located 25 km from the source region could persist for significantly longer in po-
 484 lar locations. While the deposit is expected to last longer due to reduced radiolysis at
 485 lower temperatures, ion sputtering is less sensitive to temperature variations and thus
 486 sets a lower bound on the overall erosion rate.
 487

488 Furthermore, observational limitations must be considered. As noted by Schenk
 489 (2020), image resolution near the poles is significantly degraded, with effective resolu-
 490 tion worsening to between 50 and 70 km. Such resolution constraints may have prevented
 491 the detection of polar plume deposits, even if they are more persistent than equatorial
 492 ones.
 493

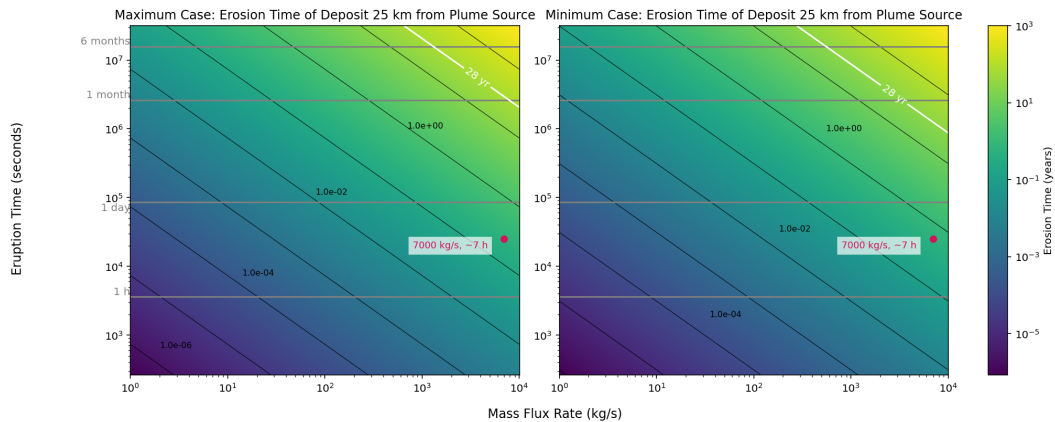


Figure 8: Combined effect of radiolysis and ion sputtering on the erosion of a plume deposit located 25 km from the source, evaluated across a range of plume eruption durations and mass fluxes. Panel (a) shows results under maximum erosion conditions on the equator (trailing hemisphere and subsolar point), while panel (b) shows the minimum erosion case (leading hemisphere and antisolar point). The two scenarios illustrate how the geographic variability of Europa's surface environment leads to differences in erosion timescales.

493 Figure 8 introduces the combined effect of radiolysis and sputtering on a plume de-
 494 posit located 25 km from the source. Panels (a) and (b) correspond to the maximum and
 495 minimum erosion scenarios at the equator, respectively, defined by the most and least
 496 erosive combinations of hemisphere and surface temperature (see Table 1). The total ero-
 497 sion differs by approximately one order of magnitude: in the maximum erosion case (Panel
 498 (a) in Figure 8), a plume with a mass flux of 10,000 kg/s active for one year survives
 499 for \sim 100 years, whereas in the equatorial minimum erosion case (Panel (b) in Figure
 500 8), the same deposit can last up to \sim 1,000 years.

501 Although this difference is non-negligible, both timescales remain extremely short
 502 in a geological context. Given Europa's estimated surface age of 60 millions years, nei-
 503 ther deposit (a) nor (b) would remain detectable after erosion, even in the most favourable
 504 scenario.

505 However, for a scenario consistent with the observed plume by HST (plume of 7,000
 506 kg/s active for ~ 7 h), the deposit lifetime is significantly shorter. In the maximum ero-
 507 sion case at the equator, the deposit survives ~ 3 months, while in the minimum ero-
 508 sion case at the equator it persists for ~ 7 months. These short timescales indicate that
 509 any deposits formed under such conditions would erode from this location within the 28
 510 year observational window used in Schenk (2020), providing a plausible explanation for
 511 the non-detection of plume deposits in that study.

512 Panel (b) in Figure 8 suggests that even under the least erosive conditions, plume
 513 deposits located 25 km from their source degrade rapidly. Therefore, we recommend that
 514 future missions focus on identifying potential deposition sites early, as their persistence
 515 is limited even in favourable locations. Further studies should explore how the longevity
 516 of these deposits evolves with Europa's rotation as variations in surface temperature and
 517 ion fluxes occur, meaning that erosion rates are unlikely to remain constant (Addison
 518 et al., 2022, 2021; Breer et al., 2019; Teolis et al., 2017a; Cassidy et al., 2013; Plainaki
 519 et al., 2012). Consequently, the notion of an "average" location used in this paper must
 520 be interpreted with caution, as surface temperature and ion impact may vary substan-
 521 tially over both space and time.

522 5 Detection of deposit by future missions

523 Our findings suggest that, in order to observe any plume deposits or surface alter-
 524 ations resulting from plume activity during future missions, such as JUICE (Tosi et al.,
 525 2024) or Clipper (Pappalardo et al., 2024), observations must be both spatially targeted
 526 and temporally optimised. In particular, for instruments with a resolution limit of ap-
 527 proximately 50 km, such as those discussed in Schenk (2020), surface imaging must oc-
 528 cur within months following an eruption of an HST plume type. Beyond this time frame,
 529 the deposits are likely to be significantly eroded, disappearing in both minimum and max-
 530 imum erosion scenarios previously discussed.

531 Moreover, the geographic location of a plume plays a critical role in the longevity
 532 and detectability of the resulting deposits, due the pronounced variability in erosion rates
 533 across Europa's surface (see Section 3). To maximise the likelihood of detecting these
 534 transient features, missions could prioritise high-resolution imaging of the polar regions,
 535 where deposits may be better preserved. Repeated observations of candidate source re-
 536 gions across multiple flybys would also be essential to constrain the persistence and evo-
 537 lution of the deposit over time.

538 A direct way to sample the deposits is by means of lander missions. Landers would
 539 offer the unprecedented opportunity to analyse plume deposits directly and potentially
 540 collect in-situ data on material from the plume fallout. Basing on Model 2 results, if a
 541 lander mission were launched today and arrived at Europa by 2040, it would need to land
 542 25 km from the plume source within months of a plume eruption (assuming an HST-type
 543 event) in order to sample any remaining deposits before they are lost to erosion.

544 Overall, our results show that plume deposits erode rapidly on geological timescales.
 545 Therefore, any mission aiming to study Europa's plume activity through surface obser-
 546 vations must carefully coordinate its arrival and observation schedule with expected plume
 547 events. Targeting regions where deposits are likely to persist at the time of landing could
 548 yield valuable insights into the physical and chemical nature of the plumes, and by ex-
 549 tension, the composition and dynamics of Europa's subsurface ocean.

550 **6 Conclusion**

551 We show that large ($\gtrsim 10$ km) plume deposits on Europa are short-lived compared
 552 to the moon's average surface age, and that their persistence strongly depends on ge-
 553 ographic location due to locally varying erosion processes, specifically ion sputtering and
 554 radiolysis. This supports the hypothesis that the absence of observed plume-related sur-
 555 face changes could result from rapid erosion rather than a lack of plume activity.

556 Using two simplified models, we simulate the erosion of plume deposits under vary-
 557 ing eruption durations and mass fluxes. For a plume similar to the one observed by HST
 558 in 2012, we find that deposits located 25 km from the source are eroded within months
 559 to a year.

560 These results highlight the need for precise temporal and spatial targeting in fu-
 561 ture surface imaging campaigns. Missions such as JUICE and Europa Clipper benefit
 562 from prioritizing high-resolution imaging of polar and leading hemisphere regions, where
 563 erosion rates are lower and the potential for deposit preservation is highest. Assuming
 564 an HST-type event, flybys should have a resolution better than 50 km and conduct imag-
 565 ing within months of a plume eruption in order to sample any remaining deposits be-
 566 fore they are lost to erosion. Repeated flybys over suspected source regions can help con-
 567 strain surface change timescales. For lander missions, deposit detection 25 km away from
 568 the source requires arrival within months of a plume eruption for HST-like events.

569 Future work can expand this framework by incorporating surface transport dynam-
 570 ics, spectral detectability thresholds, and coupled erosion-plume models to further re-
 571 fine our understanding of Europa's surface activity.

572 **Open Research Section**

573 The code to make the figures can be accessed in Casado-Anarte and Huybrighs (2025)
 574 archived on Zenodo under an open license and with a doi.

575 **Acknowledgments**

576 We thank the members of the DIAS Planetary Magnetospheres Group and Paul Schenk
 577 for useful discussions. The work of MCA, HH and SC at DIAS was supported by Taighde
 578 Éireann - Research Ireland award 22/FFP-P/11545 to Caitríona Jackman and HH. The
 579 work of MCA was supported by a DIAS Planetary Science Internship funded by Taighde
 580 Éireann in 2024 and 2025. The work of HH was supported by a DIAS Research Fellow-
 581 ship in Astrophysics. HH acknowledges the Royal Irish Academy which enabled a research
 582 visit that supported this study through the 2024-2025 Charlemont Grant Scheme. The
 583 work of NV was supported by a DIAS Planetary Science internship funded by Taighde
 584 Éireann in 2025. IL's stay at DIAS was enabled through the Trinity College Dublin final-
 585 year Capstone Project in 2023.

586 **References**

587 Addison, P., Liuzzo, L., Arnold, H., & Simon, S. (2021). Influence of europa's time-
 588 varying electromagnetic environment on magnetospheric ion precipitation and
 589 surface weathering. *Journal of Geophysical Research: Space Physics*, 126(5),
 590 e2020JA029087.

591 Addison, P., Liuzzo, L., & Simon, S. (2022). Effect of the magnetospheric plasma in-
 592 teraction and solar illumination on ion sputtering of europa's surface ice. *Jour-*
 593 *nal of Geophysical Research: Space Physics*, 127(2), e2021JA030136.

594 Archinal, B. A., A'Hearn, M. F., Bowell, E., Conrad, A., Consolmagno, G. J.,
 595 Courtin, R., ... others (2011). Report of the iau working group on carto-

graphic coordinates and rotational elements: 2009. *Celestial Mechanics and Dynamical Astronomy*, 109(2), 101–135.

Arnold, H., Liuzzo, L., & Simon, S. (2019). Magnetic signatures of a plume at europa during the galileo e26 flyby. *Geophysical Research Letters*, 46(3), 1149–1157.

Becker, H. N., Lunine, J. I., Schenk, P. M., Florence, M. M., Brennan, M. J., Hansen, C. J., ... Alexander, J. W. (2023). A complex region of europa's surface with hints of recent activity revealed by juno's stellar reference unit. *Journal of Geophysical Research: Planets*, 128(12), e2023JE008105.

Berg, J., Goldstein, D., Varghese, P., & Trafton, L. (2016). Dsmc simulation of europa water vapor plumes. *Icarus*, 277, 370–380.

Bierhaus, E., Zahnle, K., & Chapman, C. (2009). Europa's crater distributions and surface ages. *Europa*, 161.

Boccelli, S., Carberry Mogan, S., Johnson, R., & Tucker, O. (2025). Sealing europa's vents by vapor deposition: An order-of-magnitude study. *Planetary and Space Science*, 263, 106136. Retrieved from <https://www.sciencedirect.com/science/article/pii/S0032063325001035> doi: <https://doi.org/10.1016/j.pss.2025.106136>

Breer, B. R., Liuzzo, L., Arnold, H., Andersson, P. N., & Simon, S. (2019). Energetic ion dynamics in the perturbed electromagnetic fields near europa. *Journal of Geophysical Research: Space Physics*, 124(9), 7592–7613.

Casado-Anarte, M., & Huybrighs, H. L. F. (2025). Water plume deposits on europa are short lived [software]. *Zenodo*. Retrieved from <https://doi.org/10.5281/zenodo.16780641> doi: 10.5281/zenodo.16780641

Cassidy, T., Paranicas, C., Shirley, J., Dalton III, J., Teolis, B., Johnson, R., ... Hendrix, A. (2013). Magnetospheric ion sputtering and water ice grain size at europa. *Planetary and Space Science*, 77, 64–73.

Chyba, C. F., & Phillips, C. B. (2002). Europa as an abode of life. *Origins of Life and Evolution of the Biosphere*, 32(1), 47–67.

Dayton-Oxland, R., Huybrighs, H. L., Winterhalder, T. O., Mahieux, A., & Goldstein, D. (2023). In-situ detection of europa's water plumes is harder than previously thought. *Icarus*, 395, 115488.

Fagents, S. A. (2003). Considerations for effusive cryovolcanism on europa: The post-galileo perspective. *Journal of Geophysical Research: Planets*, 108(E12).

Fagents, S. A., Greeley, R., Sullivan, R. J., Pappalardo, R. T., Prockter, L. M., Team, G. S., et al. (2000). Cryomagmatic mechanisms for the formation of rhadamanthys linea, triple band margins, and other low-albedo features on europa. *Icarus*, 144(1), 54–88.

Famá, M., Shi, J., & Baragiola, R. (2008). Sputtering of ice by low-energy ions. *Surface Science*, 602(1), 156–161.

Galli, A., Vorburger, A., Wurz, P., Cerubini, R., & Tulej, M. (2018). First experimental data of sulphur ions sputtering water ice. *Icarus*, 312, 1–6.

Hand, K. P., Chyba, C. F., Priscu, J. C., Carlson, R. W., & Nealson, K. H. (2009). Astrobiology and the potential for life on europa. *Europa*, 589, 629.

Hansen, C., Ravine, M., Schenk, P., Collins, G., Leonard, E., Phillips, C., ... Jónsson, B. (2024). Juno's junocam images of europa. *The Planetary Science Journal*, 5(3), 76.

Huybrighs, H. L., Futaana, Y., Barabash, S., Wieser, M., Wurz, P., Krupp, N., ... Vermeersen, B. (2017). On the in-situ detectability of europa's water vapour plumes from a flyby mission. *Icarus*, 289, 270–280.

Jia, X., Kivelson, M. G., Khurana, K. K., & Kurth, W. S. (2018). Evidence of a plume on europa from galileo magnetic and plasma wave signatures. *Nature Astronomy*, 2(6), 459–464.

Johnson, R., Burger, M., Cassidy, T., Leblanc, F., Marconi, M., & Smyth, W. (2009). Composition and detection of europa's sputter-induced atmosphere.

706 domes on europa. *Icarus*, 284, 477–488.

707 Quick, L. C., & Hedman, M. M. (2020). Characterizing deposits emplaced by cryo-
708 volcanic plumes on europa. *Icarus*, 343, 113667.

709 Roth, L., Retherford, K. D., Ivchenko, N., Schlatter, N., Strobel, D. F., Becker,
710 T. M., & Grava, C. (2017). Detection of a hydrogen corona in hst ly α images
711 of europa in transit of jupiter. *The Astronomical Journal*, 153(2), 67.

712 Roth, L., Saur, J., Retherford, K. D., Strobel, D. F., Feldman, P. D., McGrath,
713 M. A., & Nimmo, F. (2014). Transient water vapor at europa’s south pole.
714 *science*, 343(6167), 171–174.

715 Schenk, P. M. (2020). The search for europa’s plumes: no surface patterns or
716 changes 1979–2007? *The Astrophysical Journal Letters*, 892(1), L12.

717 Schenk, P. M., Chapman, C. R., Zahnle, K., & Moore, J. M. (2004). Ages and inte-
718 riors: The cratering record of the galilean satellites. *Jupiter: The planet, satel-
719 lites and magnetosphere*, 2, 427.

720 Steinbrügge, G., Voigt, J. R., Wolfenbarger, N. S., Hamilton, C., Soderlund, K.,
721 Young, D., ... Schroeder, D. M. (2020). Brine migration and impact-
722 induced cryovolcanism on europa. *Geophysical Research Letters*, 47(21),
723 e2020GL090797.

724 Szalay, J., Allegri, F., Ebert, R., Bagenal, F., Bolton, S., Fatemi, S., ... others
725 (2024). Oxygen production from dissociation of europa’s water-ice surface.
726 *Nature astronomy*, 1–10.

727 Teolis, B., Wyrick, D., Bouquet, A., Magee, B., & Waite, J. (2017a). Plume and sur-
728 face feature structure and compositional effects on europa’s global exosphere:
729 Preliminary europa mission predictions. *Icarus*, 284, 18–29.

730 Teolis, B., Wyrick, D., Bouquet, A., Magee, B., & Waite, J. (2017b, Mar). Plume
731 and surface feature structure and compositional effects on europa’s global
732 exosphere: Preliminary europa mission predictions. *Icarus*, 284, 18–29. Re-
733 trieval from <http://dx.doi.org/10.1016/j.icarus.2016.10.027> doi:
734 10.1016/j.icarus.2016.10.027

735 Tosi, F., Roatsch, T., Galli, A., Hauber, E., Lucchetti, A., Molyneux, P., ... oth-
736 ers (2024). Characterization of the surfaces and near-surface atmospheres of
737 ganymede, europa and callisto by juice. *Space science reviews*, 220(5), 59.

738 Tseng, W.-L., Lai, I.-L., Hsu, H.-W., Ip, W.-H., & Wu, J.-S. (2025). Surface depo-
739 sition of icy dust entrained in europa’s plumes. *The Planetary Science Journal*,
740 6(4), 90.

741 Villanueva, G., Hammel, H., Milam, S., Faggi, S., Kofman, V., Roth, L., ... others
742 (2023). Endogenous co₂ ice mixture on the surface of europa and no detection
743 of plume activity. *Science*, 381(6664), 1305–1308.

744 Vorburger, A., & Wurz, P. (2018). Europa’s ice-related atmosphere: the sputter con-
745 tribution. *Icarus*, 311, 135–145.

746 Vorburger, A., & Wurz, P. (2021). Modeling of possible plume mechanisms
747 on europa. *Journal of Geophysical Research: Space Physics*, 126(9),
748 e2021JA029690.

749 Waite, J. H., Glein, C. R., Perryman, R. S., Teolis, B. D., Magee, B. A., Miller, G.,
750 ... others (2017). Cassini finds molecular hydrogen in the enceladus plume:
751 evidence for hydrothermal processes. *Science*, 356(6334), 155–159.

752 Watanabe, N., Horii, T., & Kouchi, A. (2000). Measurements of d₂ yields from
753 amorphousd₂o ice byultraviolet irradiation at 12 k. *The Astrophysical Journal*,
754 541(2), 772.

755 Winterhalder, T. O., & Huybrighs, H. L. (2022). Assessing juice’s ability of in situ
756 plume detection in europa’s atmosphere. *Planetary and Space Science*, 210,
757 105375.

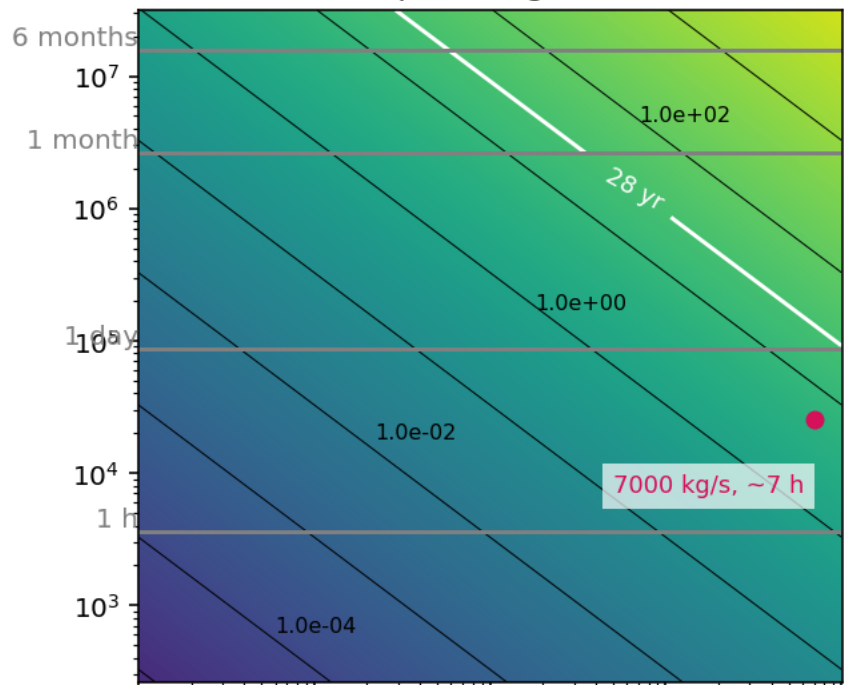
758 Yoffe, G., Duer-Milner, K., Nordheim, T. A., Halevy, I., & Kaspi, Y. (2025). Flu-
759 orescent biomolecules detectable in near-surface ice on europa. *Astrobiology*,
760 25(5), 359–366.

761 Zahnle, K., Schenk, P., Levison, H., & Dones, L. (2003). Cratering rates in the outer
762 solar system. *Icarus*, 163(2), 263–289.

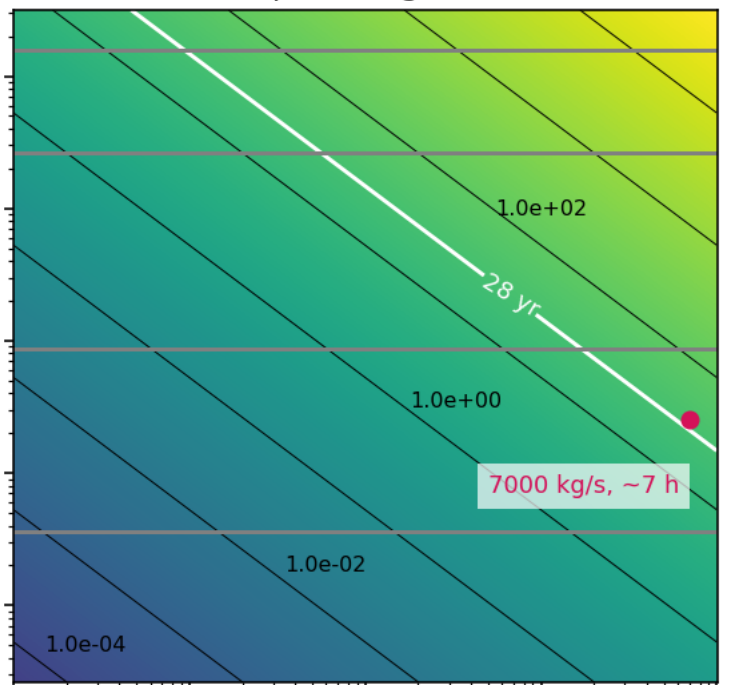
Figure 7.

Eruption Time (seconds)

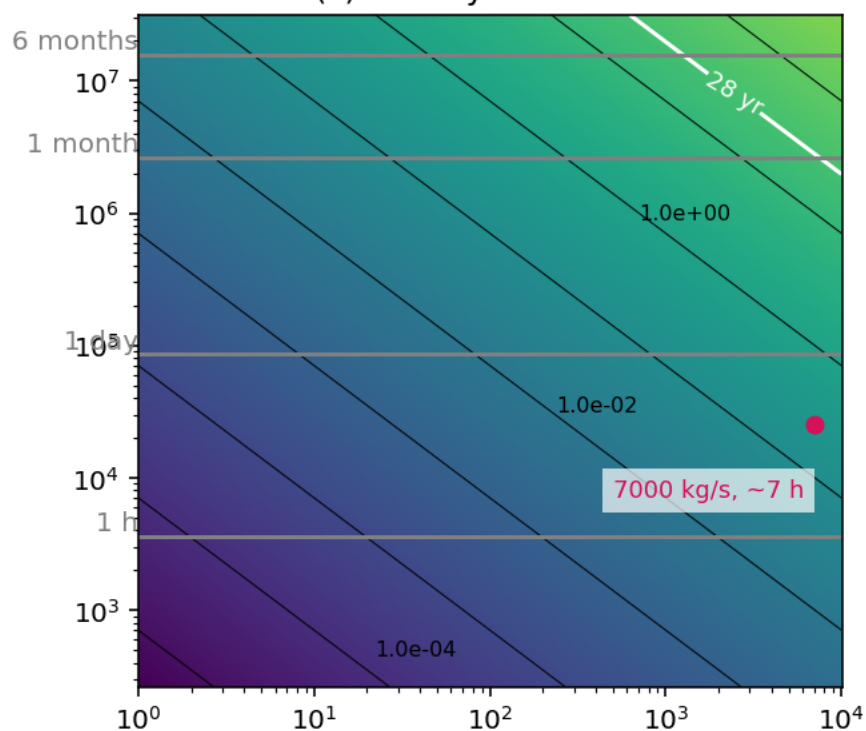
(a) Sputtering at T.H.



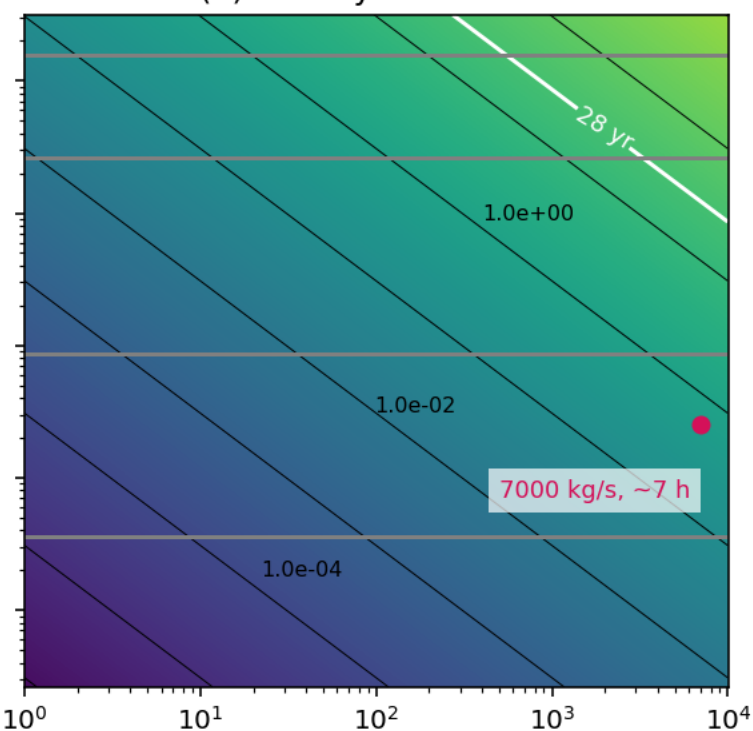
(b) Sputtering at L.H.



(c) Radiolysis at S.S.P.



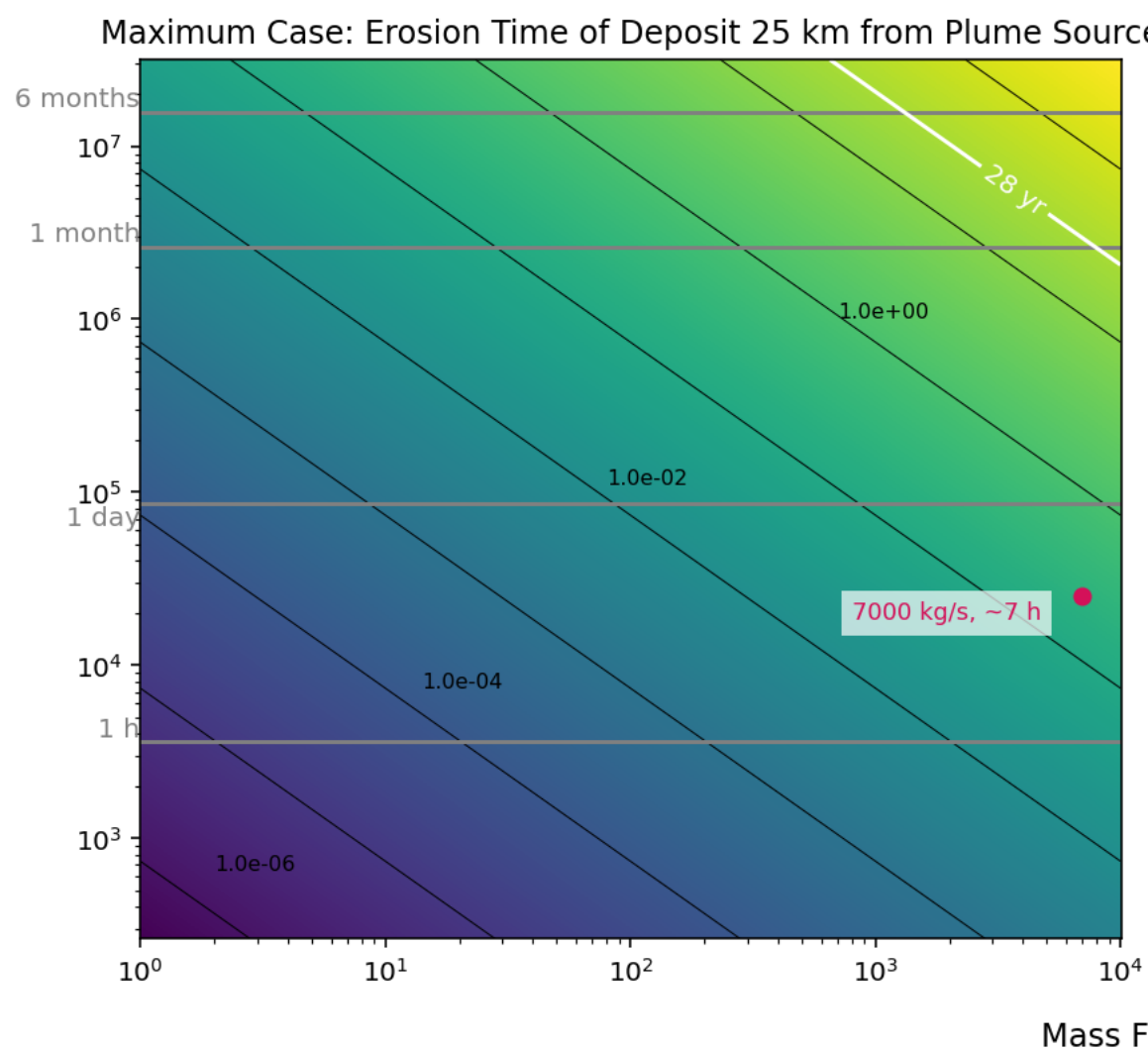
(d) Radiolysis at A.S.P.



Mass Flux Rate (kg/s)

Figure 8.

Maximum Case: Erosion Time of Deposit 25 km from Plume Source



e Minimum Case: Erosion Time of Deposit 25 km from Plume Source

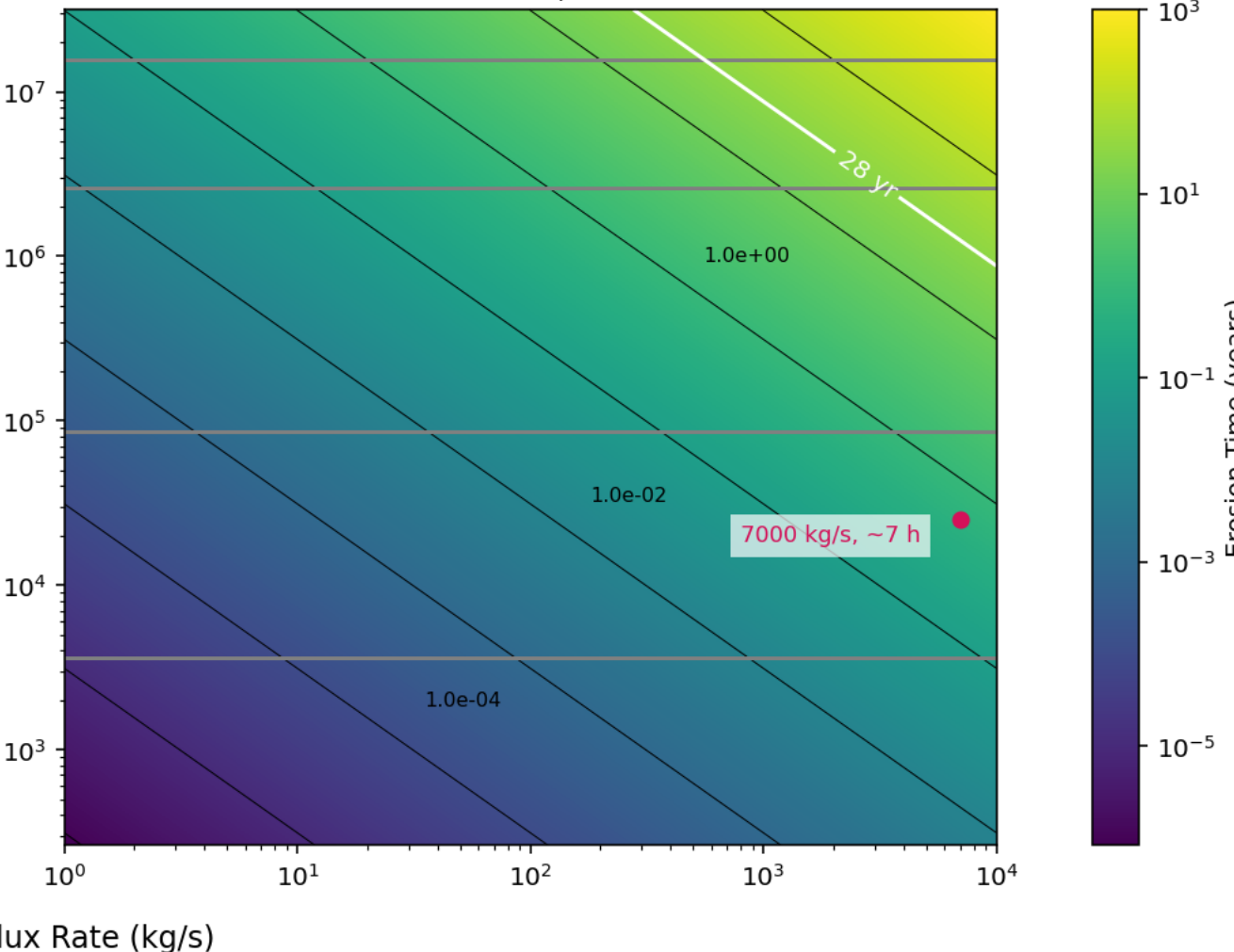


Figure 2.

Spatial Distribution of H₂O in Plume

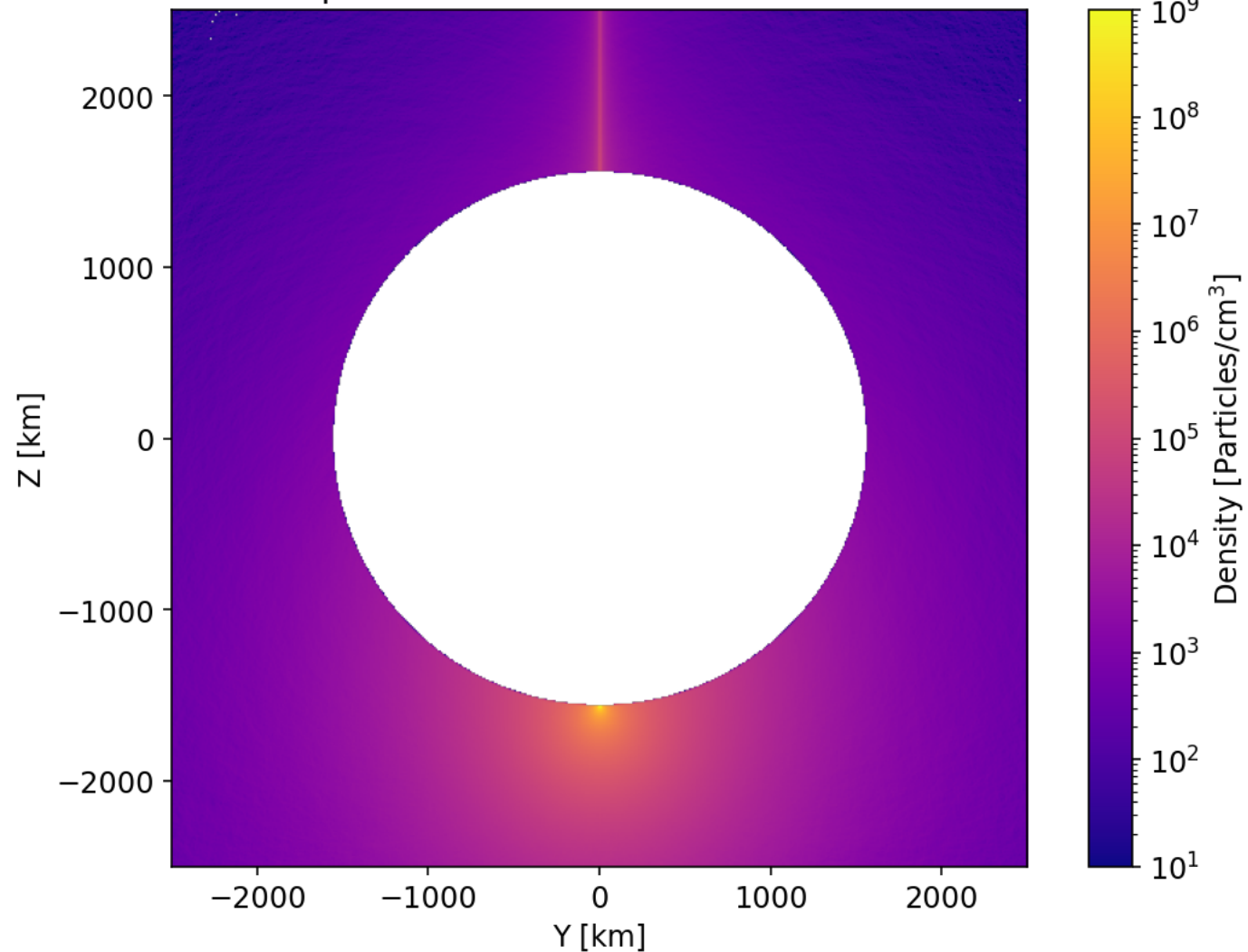


Figure 1.

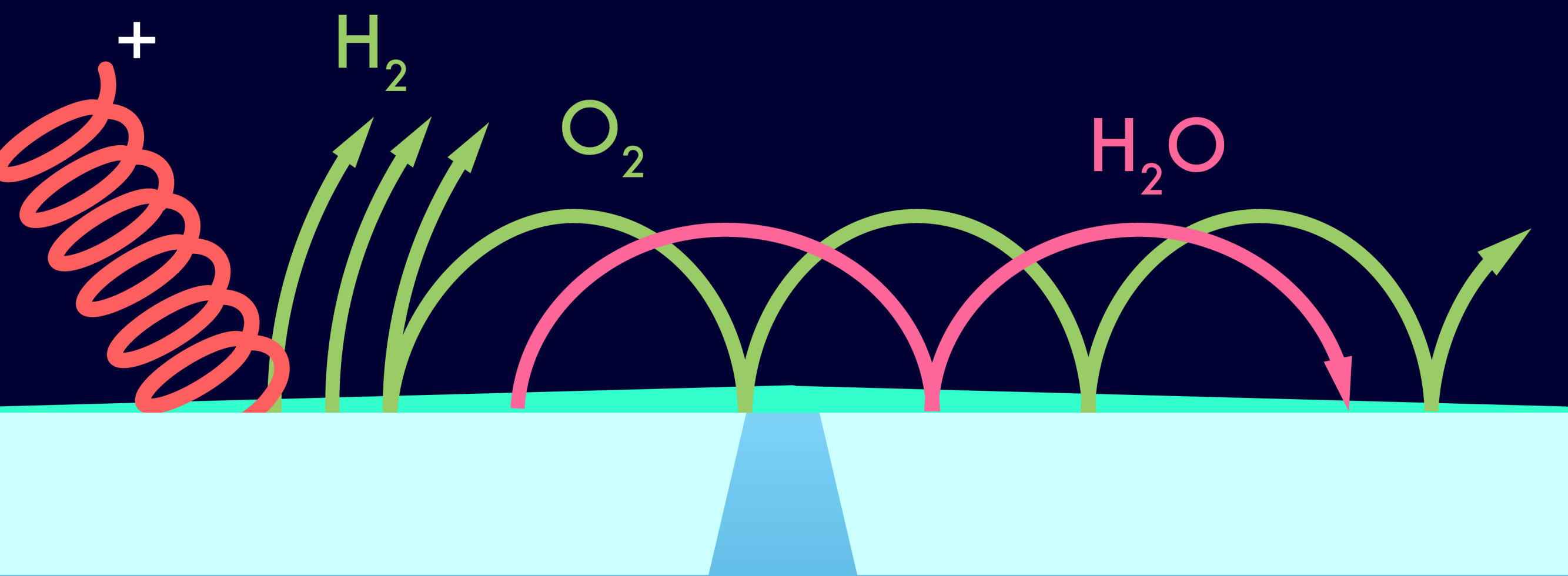
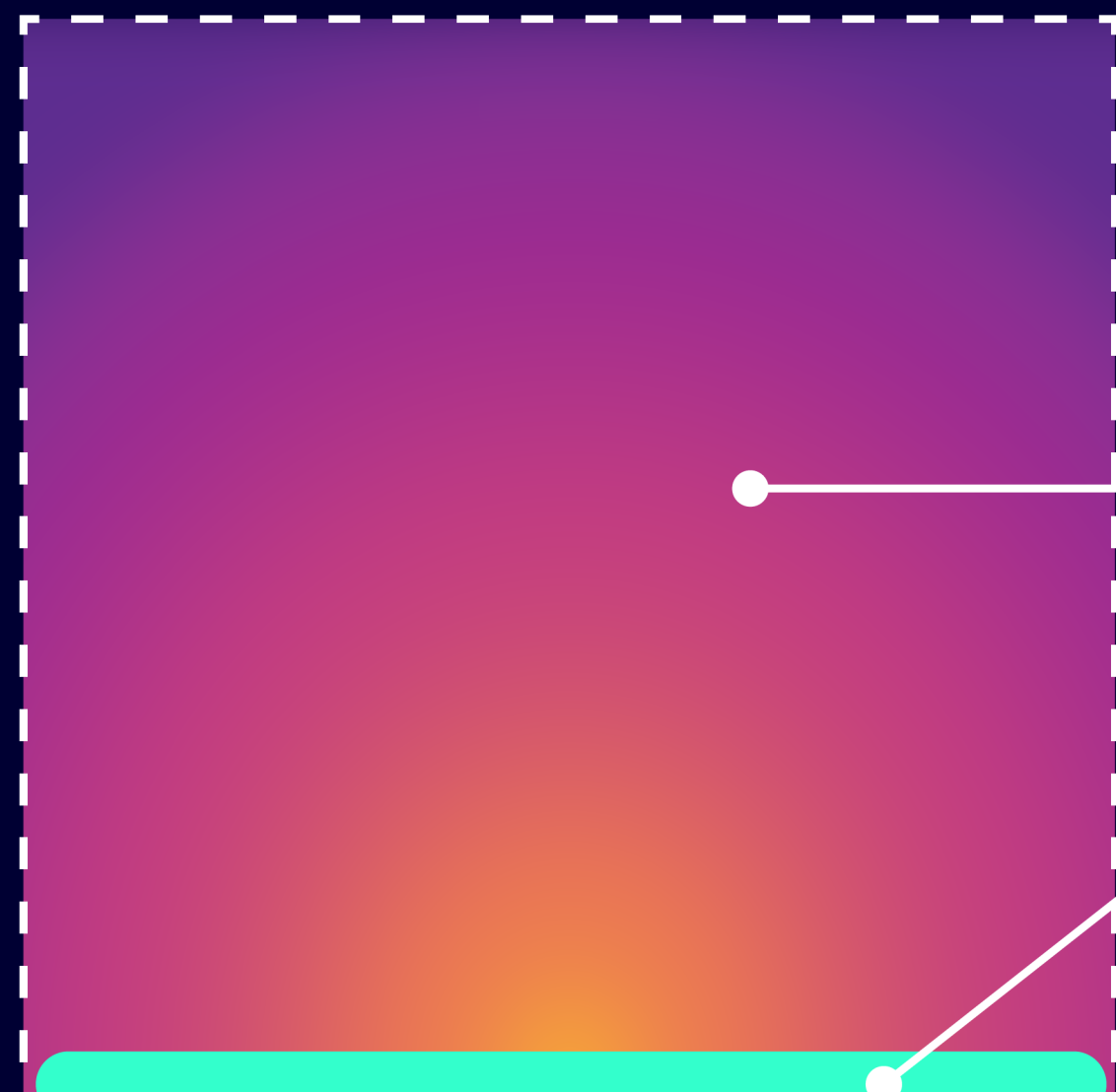


Figure 3.

10 x 10 km



H_2O

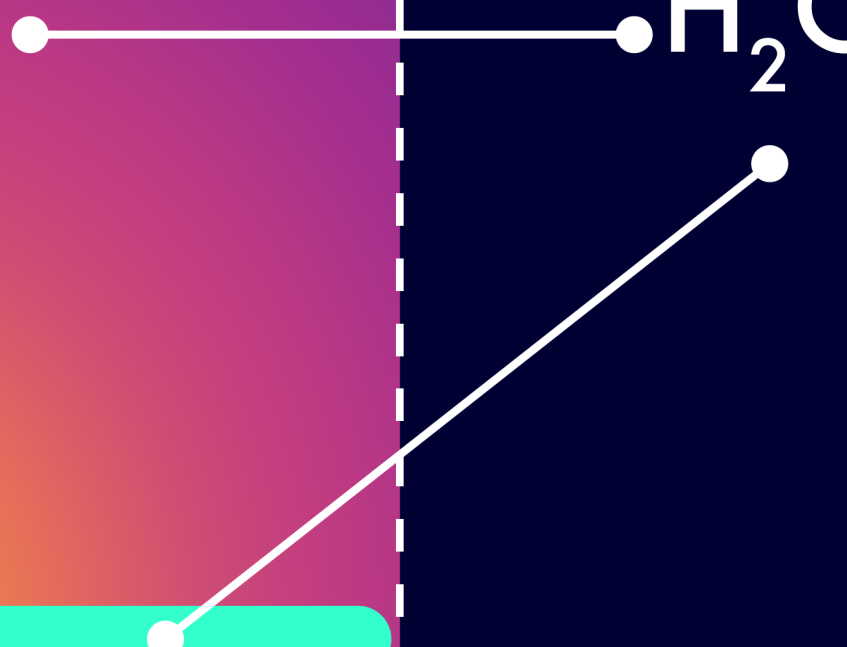


Figure 4.

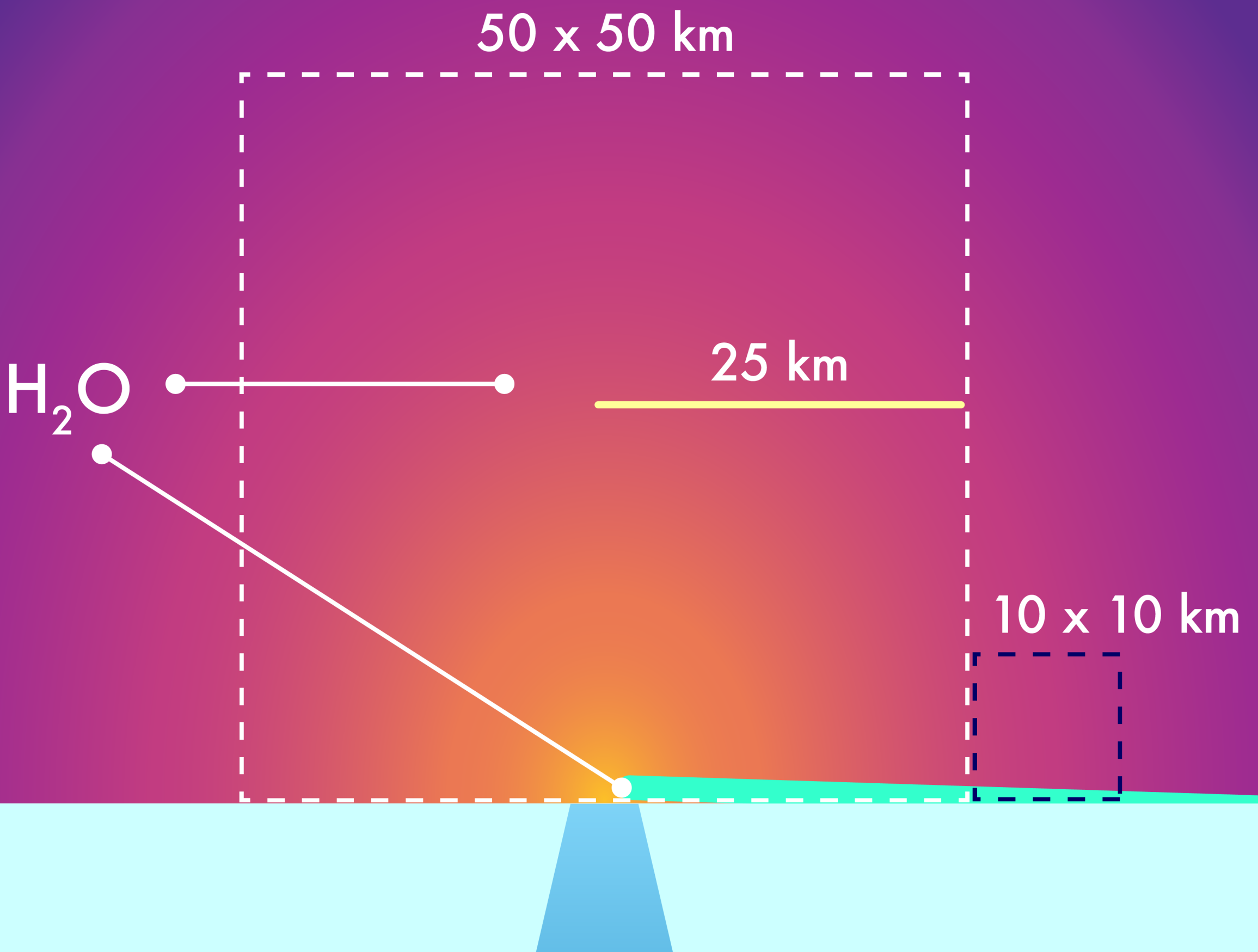


Figure 6.

Average Erosion Time of Deposit 25 km Away from Plume Source

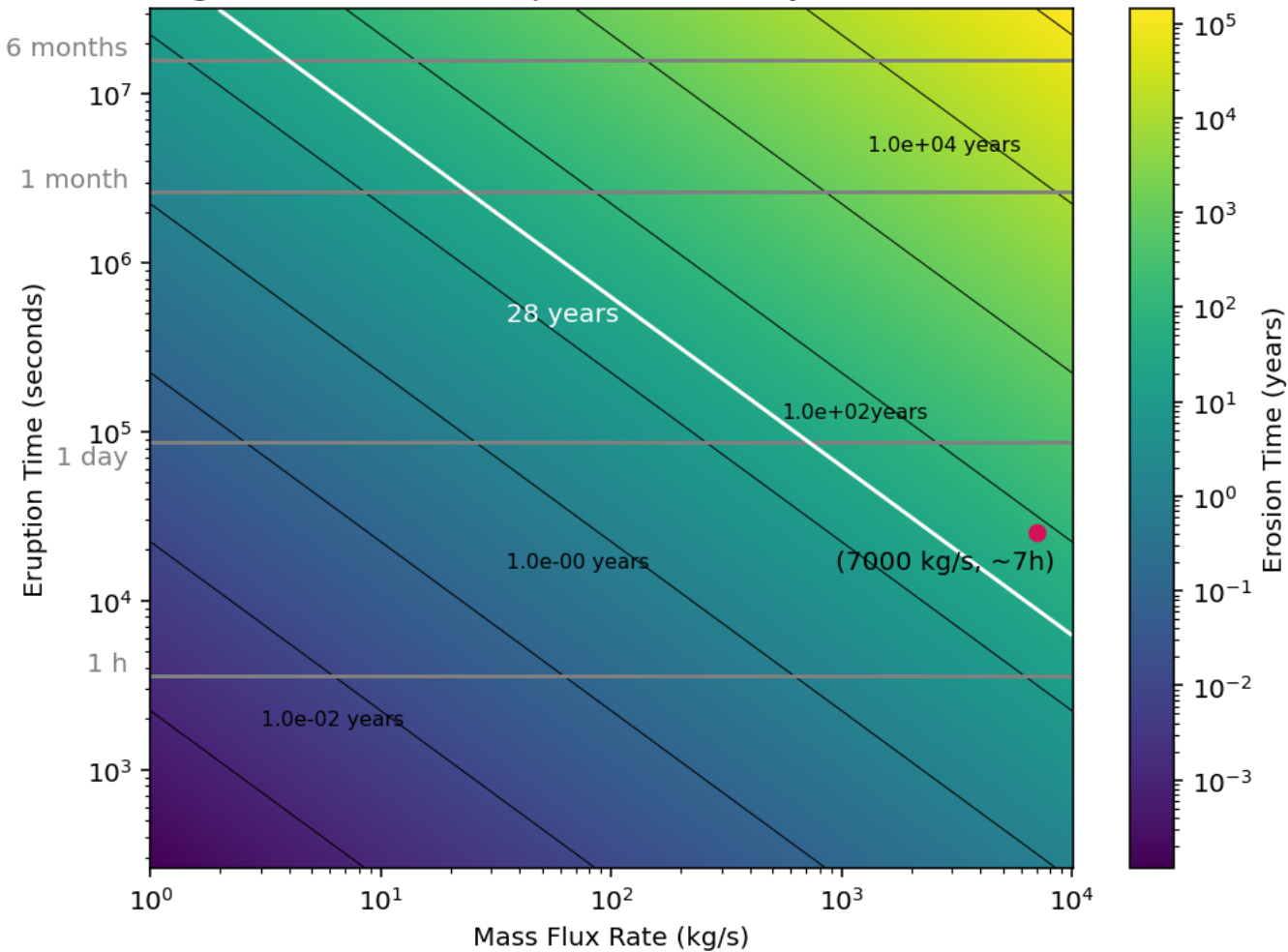


Figure 5.

Model 1: Erosion Time of Deposit due to Sputtering and Radiolysis

